FACULTY OF INFORMATION TECHNOLOGY AND ELECTRICAL ENGINEERING

DEGREE PROGRAMME IN ELECTRONICS AND COMMUNICATIONS ENGINEERING

MASTER'S THESIS

Cell Measurement in 5G Unlicensed Spectrum

Author	Joni Huttula
Supervisor	Markku Juntti
Second Examiner	Janne Lehtomäki
Technical Advisor	Lauri Anttonen

May 2022

Huttula J. (2022) Cell Measurement in 5G Unlicensed Spectrum. University of Oulu, Faculty of Information Technology and Electrical Engineering, Degree Programme in Electronics and Communications Engineering. Master's Thesis, 65 p.

ABSTRACT

The objective of the thesis is to implement a firmware for cell measurement in an unlicensed spectrum. As a part of the thesis, theory for downlink physical layer and resources are reported as they are related to the implementation. Also, a short introduction to New radio cell measurement in licensed and unlicensed spectrum are presented and the main differences between those radio access technologies are shown. The biggest differences, but also the most challenging parts between licensed and unlicensed spectrum measurements are Listen-before-talk and expanded quasi co-location assumption. Listen-before-talk is used to evaluate the state of the channel and expanding quasi co-location assumption to all synchronization blocks to make time shift possible for the block.

The performance of the implementation was measured in two different ways. The first way was to track a data and a program memory usage behave. The second way was to measure a cycle usage to see how central processing unit load behave in comparison to New radio.

The results show clearly that the data memory usage increases linearly as a function of the candidate locations. Also, the program memory size increases about 5%. The results of the program memory show that the implementation reuses a lot of the New radio code as this new access technology does not increase the size of the program memory much. This kind of the results can also be seen with the cycle usage measurements. When it was measured only one candidate location in the unlicensed spectrum, the cycle usage increases about 10% when comparing to the New radio. However, the cycle usage did not increase linearly when more candidate location was measured. It was observed that the more candidate locations were measured, the less one candidate location measurement consumes the cycles on average. The observation supports the conclusion that the implementation reuses a lot of New radio code and there is a lot of the common code.

Key words: NR, new radio, NR-U, secondary synchronization signal, unlicensed spectrum, quasi co-location.

Huttula J. (2022) Solumittaus lisensoimattomilla 5G-taajuuksilla. Oulun yliopisto, tieto- ja sähkötekniikan tiedekunta, elektroniikan ja tietoliikennetekniikan tutkinto-ohjelma. Diplomityö, 65 p.

TIIVISTELMÄ

Tavoite opinnäytetyölle on toteuttaa laiteohjelmisto, joka suorittaa solumittausta lisensoimattomilla 5G-taajuuksilla. Osana opinnäytetyötä on esitetty teoriaa siltä osin kuin se on toteutuksen kannalta olennaista. Teoria käsittelee 5G-yhteyden alalinkin fyysisen kerroksen eri osia ja resursseja sekä solumittausta lisensoidulla ja lisensoimattomilla 5G-taajuuksilla kuin myös niiden eroja solumittauksessa. Suurimmat erot lisensoidulla ja lisensoimattomilla 5G-taajuuksien solumittauksissa, ja samalla myös pääasiallinen haaste syntyi kuuntele ennen puhetta -teknologiasta sekä näennäisen yhteissijoittamisen käsitteen laajentamisesta. Kuuntele ennen puhetta -teknologiaa käytetään kanavan tilan seurantaan. Näennäisen yhteissijoittamisen käsiteen laajentaminen mahdollistaa synkronisointi lohkon siirtämisen aikatasolla suhteessa muihin synkronisointi lohkoihin.

Toteutuksen suoritustasoa mitataan kahdella eri tavalla. Ensimmäinen tapa on seurata muistin käyttäytymistä solumittauksessa sekä toteutuksesta syntyvää ohjelmistomuistin kasvua. Toinen tapa seurata suorituskykyä on mitata syklejä. Syklejä mittaamalla saadaan tietää kuinka paljon prosessori kuormittuu mittausten aikana.

Tulokset osoittavat, että muistin kulutus solumittauksessa kasvaa lineaarisesti ehdokaspaikkojen funktiona. Myös ohjelmistomuistin koko kasvaa noin 5%. Ohjelmistomuistin kasvusta voidaan päätellä, että laiteohjelmisto uudelleenkäyttää paljon vanhaa lisensoidun taajuuden mittausohjelmistoa, jolloin uuden radiopääsytekniikan toteutus ei juurikaan nosta ohjelmiston kokoa. Saman kaltaisia tuloksia voidaa myös huomata syklien mittauksessa. Kun mitattiin yhden lisensoimattoman taajuuden ehdokaspaikan mittauksesta aiheutuvaa syklien kulutusta, huomattiin sen nousevan 10% verrattuna vastaavaan lisensoidun taajuuden mittaukseen. Kuitenkin, kun suoritettiin useamman ehdokaspaikan solumittaus, huomattiin, että syklimäärä itseasiassa laski per ehdospaikan mittaus. Tästä voidaan päätellä, että kaikki syklit eivät kertaudu jokaisessa ehdokaspaikan mittauksessa, vaan ohjelmisto sisältää paljon niin sanottua yleistä ohjelmistoa. Mitä enemmän ehdospaikkoja on mitattavana, sitä vähemmän yksi mittauspaikka maksaa.

Avainsanat: NR, uusradio, NR-U, toissijainen synkronointisignaali, lisensoimaton taajuus, näennäinen yhteissijoittaminen.

TABLE OF CONTENTS

FOREWORD

The objective of the thesis was to study cell measurement in 5G NR unlicensed spectrum which have been introduced in 3GPP Release 16. 5G NR in the unlicensed spectrum offers a new radio access to create new products and extend 5G NR experience for the indoor users. Based on the research, the firmware implementation to 5G modem were created. The research and the implementation were done to MediaTek Wireless Finland Oy from September 2021 to May 2022.

At first, I want to thank my technical advisor Lauri Anttonen for a great help and guidance through the research and thesis work. I also want to thank my manager Jukka Rahikkala for the opportunity to join to the team and to do my thesis with this interest topic. Furthermore, my colleague Ilmari Maskulainen deservers great thanks for answering to all my questions. I also want to thank my supervisor Markku Juntti and my second examiner Janne Lehtomäki for great and seamless cooperation to get this thesis done.

Oulu, May 4, 2022

Joni Huttula

LIST OF ABBREVIATIONS AND SYMBOLS

3GPP	Third-Generation Partnership Project
5G NR	Fifth generation new radio
AoD	Angle-of-departure
CA	Carrier aggregation
CAPC	Channel access priority class
CFO	Carrier frequency offset
CM	Cell measurement
CORESET	Control resource set
COT	Channel occupancy time
CP	Cyclic prefix
CP-OFDM	Cyclic prefix orthogonal frequency-division multiplexing
CPU	Central processing unit
CQI	Channel quality indicator
CSI	Channel-state information
CSI-RS	Channel-state information reference signal
DC	Dual Connectivity
DCI	Downlink control information
DFS	Dynamic frequency selection
DFTS-OFDM	Discrete Fourier transform spread orthogonal frequency-division multiplexing
DL	Downlink
DM-RS	Demodulation reference signal
DSP	Digital signal processing
EIRP	Equivalent isotropically radiated
eNB	eNodeB, LTE base station
ETSI	European Telecommunications Standards Institute
FDD	Frequency-division duplex
FFO	Fractional frequency offset
FFT	Fast Fourier transform
FR	Frequency reuse
FR1	Frequency range 1
FR2	Frequency range 2
FW	Firmware
gNB	gNodeB, 5G NR base station
HARQ	Hybrid automatic repeat request
ID	Identity
IEEE	Institute of Electrical and Electronics Engineers
IFO	Integer frequency offset
IMS	IP multimedia subsystem
Io	Total received power density
ISI	Intersymbol interference
KPI	Key performance indicator
L1	Layer 1
L3	Layer 3
LBT	Listen-before-talk
LTE	Long-term evolution
MCOT	Maximum channel occupancy time

MIB	Master information block
MIMO	Multiple-input multiple-output
mmWave	Millimetre wave
MRTD	Maximum receive timing differences
MU	Measurement unit
NR-U	New radio unlicensed
NR	New radio
OCB	Occupied channel bandwidth
OFDM	Orthogonal frequency-division multiplexing
PBCH	Physical broadcast channel
PCell	Primary cell
PCI	Physical cell identity
PDSCH	Physical downlink shared channel
PDCCH	Physical downlink control channel
PMI	Precoder-matrix indicator
PRS	Positioning reference signal
PSCell	Primary secondary cell
PSD	Power spectra density
PSS	Primary synchronization signal
PT-RS	Phase-tracking reference signal
QCL	Quasi co-located
RAT	Radio access technology
RB	Resource block
RI	Rank indicator
RSRP	Reference signal received power
RSRQ	Reference signal received quality
RSSI	Received signal strength indicator
RTT	Round trip time
SCell	Secondary cell
SCS	Subcarrier space
SIB1	System information block 1
SIC	Successive interference cancellation
SINR	Reference signal-to-noise-plus-interference ratio
SMTC	SS/PBCH block measurement time configuration
SS/PBCH	See SSB
SSB	Synchronization signal block
SSS	Secondary synchronization signal
STO	Symbol time offset
TDD	Time-division duplex
TDOA	Time difference of arrival
TS	Technical specification
UE	User equipment
UL	Uplink
UNII	Unlicensed national information infrastructure

$\mathbb{D}$	The interval of subcarrier indices
d_{PSS}	PSS M-sequence
d_{SSS}	SSS Gold sequence

$C(\theta, i)$	Joint estimation for timing offset and cell ID sector
CW_{p}	Contention window for given channel access priority class
$CW_{\mathrm{min,p}}$	Minimum contention window for given channel access priority class
$CW_{\mathrm{max,p}}$	Maximum contention window for given channel access priority class
$D_{\mathrm{w}}(k)$	Local differential PSS function per possible cell ID sector
$\hat{g}_{\mathrm{SSS}}$	Estimated cell ID group
$\hat{\imath}$	The value of estimated cell ID sector.
m_{p}	Sensing slot
N	A random uniformly distributed number between 0 and CW_{p}
N_{f}	The FFT size of 5G NR
$N_{\mathrm{f,ref}}$	The FFT size of LTE
$N_{\mathrm{CP,l}}^{\mu}$	Cyclic prefix length per subcarrier spacing
N_{u}^{μ}	Useful OFDM symbol time
$N_{\mathrm{ID}}^{(1)}$	Cell identity groups
$N_{\mathrm{ID}}^{(2)}$	Cell ID sector
$N_{\mathrm{ID}}^{\mathrm{cell}}$	Serving cell ID
N_{FFT}	The number of fast Fourier transform without cyclic prefix
$N_{\mathrm{slot}}^{\mathrm{frame},\mu}$	Slots per frame for certain subcarrier spacing
$N_{\mathrm{subframe}}^{\mathrm{frame},\mu}$	Subframes per frame for certain subcarrier spacing
$N_{\mathrm{symb}}^{\mathrm{frame},\mu}$	Symbols per frame for certain subcarrier spacing
$N_{\mathrm{DM-RS}}^{\mathrm{PBCH}}$	The index of DM-RS sequence
$N_{\mathrm{SSB}}^{\mathrm{QCL}}$	QCL value
$N_{\mathrm{SC}}^{\mathrm{RB}}$	The number of subcarriers in resource block
$N_{\mathrm{grid,x}}^{\mathrm{size},\mu}$	The size of the resource grid per subcarrier spacing
$N_{\mathrm{symb}}^{\mathrm{slot}}$	Symbols per slots
$N_{\mathrm{slot}}^{\mathrm{subframe},\mu}$	Slots per subframe for certain subcarrier spacing
p	The class of channel access priority
$p_{\mathrm{i}}^{*}(k)$	PSS sequence with cell ID sector i
$r(.)$	Received signal
$S_{\mathrm{c}}(k)$	Predefined SSS sequence per cell ID group
T_{c}	Basic time unit in 5G NR
T_{d}	Defer duration
T_{f}	Frame duration
T_{fd}	Duration for defer duration
$T_{\mathrm{mcot,p}}$	The duration of maximum channel occupancy time
T_{s}	Basic time unit in LTE
T_{sf}	Subframe duration
$\mathrm{T_{sl}}$	Sensing slot duration
$T_{\mathrm{symb,l}}^{\mu}$	The duration of symbol length per subcarrier spacing
$\hat{u}$	Estimated cell ID sector
$\mathrm{X_{Thresh}}$	Energy detection threshold
$X_{\mathrm{Tresh\_max}}$	Maximum energy detection threshold
$Y_{\mathrm{l}}(k)$	Received signal in kth subcarrier at lth symbol
$\bar{Y}_{\mathrm{l}}(k)$	Received differential PSS function at lth symbol

$(k,l)_{\mathrm{p},\mu}$	Resource element, where k is the index of subcarrier, l is the index of OFDM symbol, p is antenna port and μ is used SCS
$\alpha(\theta)$	The energy part of timing offset estimation
$\gamma(\theta)$	The correlation part of timing offset estimation
Δf	Subcarrier spacing
$\Delta f_{\max}$	The maximum subcarrier spacing of 5G NR
Δf_{ref}	The maximum subcarrier spacing of LTE
ϵ	The value of carrier frequency offset
$\hat{\epsilon}_{\mathrm{FFO}}$	The value of estimated fractional frequency offset
$\hat{\epsilon}$	The value of estimated carrier frequency offset
$\hat{\epsilon}_{\mathrm{IFO}}$	The value of estimated integer frequency offset
θ	The value of timing offset
$\hat{\theta}$	The value of estimated timing offset
κ	Ratio between T_{s} and T_{c}
μ	Subcarrier spacing configuration
ρ	The magnitude of the correlation coefficient
σ_{s}^2	Signal power
σ_{N}^2	Noise power
$\Phi_{\mathrm{PSS}}(m,w)$	Correlation function for PSS estimation
$\Phi_{\mathrm{SSS}}(c)$	Correlation function for SSS estimation
$\Re(.)$	Real part
$\angle(.)$	argument
$(.)^*$	complex conjugate

1 INTRODUCTION

Fifth generation new radio (5G NR) has come to our life widely. In July 2020, Third-Generation Partnership Project's (3GPP) Release 16 was completed and NR access for an unlicensed spectrum (NR-U) was introduced [1]. In NR-U, main goal is to provide a worldwide solution for utilizing the unlicensed spectrum which has also considered regulations of the different countries [2]. NR-U is targeted to work in 5 GHz and 6 GHz bands by using a time-division duplex (TDD) mode as Table 1 shows [2].

Table 1. Frequency ranges for unlicensed spectrum

Duplex mode	NR operating bands	Downlink and Uplink frequencies
TDD	n46	5150 MHz – 5925 MHz
TDD	n96	5925 MHz – 7125 MHz

NR-U has been designed for bands which are for free use for everyone without any cost. The unlicensed spectrum is an opposite to a licensed spectrum where the spectrum is restricted for certain network technology, for example, 5G NR. In the unlicensed spectrum, this is not the case and a device, and a network must adapt its transmissions with other technologies. European Telecommunications Standards Institute (ETSI) have created requirements to enable a fair coexistence for systems. Most well-known radio access technologies (RATs) utilizing the unlicensed spectrum in 2.4—2.4835 GHz and 5.725—5.85 GHZ frequency areas are Institute of Electrical and Electronics Engineers (IEEE) 802.11-based Wi-Fi, Bluetooth and ZigBee. To enable fair wireless medium usage, NR-U must have following technologies: a listen-before-talk (LBT), a maximum channel occupancy time (MCOT), an equivalent isotropically radiated power (EIRP) and a power spectra density (PSD), an occupied channel bandwidth (OCB), a frequency reuse (FR) and a dynamic frequency selection (DFS). [3] [4] [5]

NR-U is designed to support five different scenarios which are named from A to E. These scenarios mainly present how NR-U could be used with other access technologies as long-term evolution (LTE) and 5G NR. Figure 1 visualizes the different scenarios. Those scenarios include situations where a user equipment (UE) use carrier aggregation (CA) or dual connectivity (DC) technology when the UE is attached to a different RAT. For example, in scenario A, the UE is attached to NR and NR-U base stations by using the carrier aggregation technology. In scenario C, the UE communicates with a standalone NR-U base station and in scenario D, the UE uses both the unlicensed and the licensed spectrum so that a downlink (DL) is in the unlicensed spectrum and an uplink (UL) is in the licensed spectrum. [2] [6]

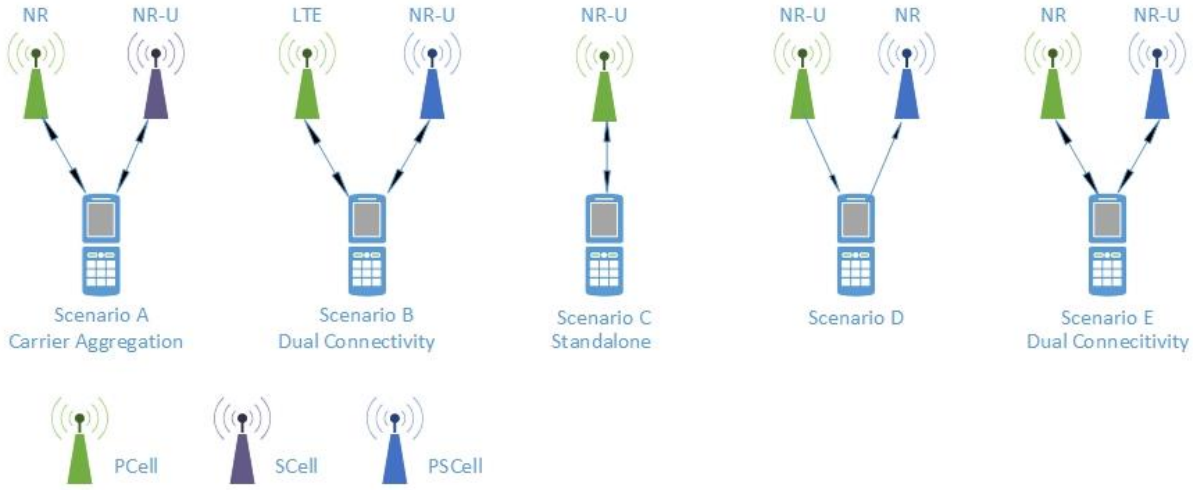

Figure 1. Different scenarios in NR-U.

A cell measurement (CM) in 5G NR is based on a synchronization signal block (SSB) and a channel-state information reference signal (CSI-RS). This thesis is focusing to the SSB measurements. SSB consists of a primary synchronization signal (PSS), a secondary synchronization signal (SSS) and a physical broadcast channel (PBCH). The UE should be able to measure a synchronization signal-based reference signal received power (RSRP), a synchronization signal-based reference signal received quality (RSRQ) and a synchronization signal-based reference signal-to-noise-plus-interference ratio (SINR). For NR-U, Release 16 introduces discovery bursts which are used to transmit the SSB and for example a system information block 1 (SIB1). Also, for 15 kHz and 30 kHz subcarrier spacing (SCS), the maximum number of the SSB locations are increased from eight to ten and twenty, respectively. However, while the number of the candidate locations is increased for NR-U, the number of the maximum transmitted SSB is not. This means more space on time domain for an SSB transmission. Also, in NR-U, the number of the supported beams no more depends on the used frequency. To allow for more flexibility, SSBs can be a quasi co-located (QCL) within a transmission window or across transmission windows. These improvements are needed as LBT could reduce the number of the SSB transmissions. [2] [3] [7] [8]

There are a couple of benefits in NR-U against Wi-Fi. NR-U opens the doors for mobility, and it also has better quality than Wi-Fi. The load of the network can be easily scaled as NR-U has, for example, a mobility offload use case. NR-U also offers a possibility for an industry and operators to build up their own private networks which could use both licensed and unlicensed spectrums. NR-U is meant to be standalone access technology, but it can also be used anchored with other existing access technologies which leads to an easy and safe network deployment. Good examples for NR-U usage could be campuses and shopping centers, where NR-U could be used to give a better 5G NR experience for the indoor users. [9] [10]

The goal of the thesis is to study how NR-U differs from NR at the cell measurement level and how differences affect to the memory usage and to the central processing unit (CPU) load of the NR modem at the firmware (FW) level. By using 3GPP technical specification (TS) 38.213 and TS 38.133 it can be shown that in the worst-case, one NR-U SSB can have 20 times as much locations as NR SSB does. This indicates, that in the worst-case scenario, there is a huge cost in memory and computing load when comparing NR and NR-U access technologies as the UE must perform measurements for all candidate locations. In an ideal case, there are only a couple of candidate locations where certain SSB could be located.

The thesis is divided into eight chapters. The first two chapters are used for the introduction of the thesis and for the introduction of the 5G NR as it is related for the thesis. In Chapter 2, the physical channels and signals of the downlink are introduced, and then the basic numerology, the frame structure and the resource grid of the 5G NR are described. After these topics, the theory of the orthogonal frequency-division multiplexing (OFDM) symbols on the time domain is introduced as well as a brief example how SSB could be detected. Chapters 3 and 4 cover the cell measurement in 5G NR and NR-U, respectively. The chapters do not go too deep into cell measurement details but describe relevant parts for implementation purposes. First, Chapter 3 presents an overview of the cell measurement and then deeper introduction for the SSB and the parameters of the cell measurement. Also, the requirements for the UE are introduced in Chapter 3. Chapter 4 focuses more on discovering the differences between NR and NR-U. The chapter introduces the used spectrum and channel access methodologies as they are the crucial part of the NR-U when thinking the fundamentals of the synchronizations. The main challenge comes from periodicity as there could be several RATs using the same wireless medium than NR-U, so the periodic SSB transmission may not be possible. Also, a QCL assumption takes a more fundamental role, and therefore it is introduced. Last topic in Chapter 4 is SSB transmission improvements. In Chapter 5, there is the short introduction of the implementation and of the NR-U related challenges and solutions. Chapter 6 is dedicated for the hypothesis of the research and the results, Chapters 7 and 8 for discussion and summary, respectively.

2 5G – NEW RADIO

This chapter mainly focuses on the introduction of the basic physical layer resources for a cell measurement. As the cell measurement is commonly performed from an SSB, physical channels and signals are introduced with frequency and time resources. Also, OFDM symbol details on the time domain introduced and the example of SSB detection is presented.

2.1 Physical Channels of Downlink

In 5G NR, there are three kind of the physical DL channels which are named a physical downlink shared channel (PDSCH), a PBCH and a physical downlink control channel (PDCCH). Their main use is to carry information from a higher layer and the information is packed into time-frequency resources. The PDSCH is mainly used for the downlink data transmission. It is controlled by another channel, the PDCCH. The PDCCH could be used, for example, to notify a slot format or to initiate a random-access procedure. This control is done with a downlink control information (DCI). The DCI also includes information about coding, modulation, resource allocation and Hybrid Automatic Repeat Request (HARQ). [11] [12] [13]

The PBCH is a broadcast channel and the part of the SSB where it is used to provide a timing information. The timing information is divided into two parts: an implicit and an explicit part. To get the implicit timing index, the PBCH has to be demodulated. At frequency range 1 (FR1) region, there are eight different scrambling patterns which can be used to identify the SSB. All bands below 7.125 GHz are counted as FR1 [14]. The explicit part of the timing information is included into the PBCH carried information and is called a master information block (MIB). The PBCH also carry a numerology and configuration for the SIB1 which include the information for connecting the UE to the base station. Also, other PDSCH and PDCCH related information are carried in the PBCH. Table 2 and Table 3 gives more information of the contents of the MIB and the SIB1, respectively. [3] [15]

Table 2. The fields of the master information block

Field	Description
System frame number	6 most significant bits of the system frame number.
Subcarrier spacing common	Subcarrier spacing for the SIB1.
SSB-subcarrier offset	The frequency domain offset between the SSB and overall resource block grid.
DM-RS TypeA position	The position of the first DM-RS for the downlink and the uplink.
PDCCH SIB1 configuration	Specifies a common CORESET. Also indicate, for example, a frequency position where to find the SSB with the SIB1.
Cell barred	Tells if the UE can connect to the base station or not.
Intra-frequency reselection	Tells if other base station on same frequency is available for the connection.

Table 3. The fields of the system information block 1

Field	Description
Cell selection info	Serving cell selection information.
Cell access related info	Cell access related information.
connection estimation failure control	Configurations for connection failure.
SI-scheduling info	Including information about SI messages.
serving cell configuration common	The configurations of the serving cell.
IMS emergency support	Indicates if the cell supports emergency calls over IP Multimedia Subsystem (IMS) in limited-service mode [16].[1]
eCall over IMS support	Indicates if the cell supports eCalls over IMS.
UE timer and constants	Timer and constant values for the UE provided by the PCell.
UAC barring info	Including the controlling information of the cell.
use full resume ID	Identifies used resume identifier and resume request message.
late non-critical extension	Octet string.
Noncritical extension	Some additional information.

2.2 Physical Signals of Downlink

There are several physical signals at the downlink, and they are called a demodulation reference signal (DM-RS), a phase-tracking reference signal (PT-RS), a positioning reference signal (PRS), a CSI-RS, a PSS and an SSS. The PT-RS is used to compensate for an oscillator phase noise as at higher carrier frequencies the local oscillator increases phase noise at a transmitter and a receiver side. The PRS is used for several positioning methods like time difference of arrival (TDOA), angle-of-departure (AoD) and round trip time (RTT). The CSI-RS is used for channel-state information (CSI) acquisition, beam management, time and frequency tracking, uplink power control and cell measurement. The DM-RS is used for demodulation. It is also the part of the SSB and is used for a coherent demodulation of the PBCH. In NR-U, the DM-RS is used to create QCL relation between the SSBs within a discovery transmission burst. The PSS and the SSS are used to synchronize the UE and a base station. For cell measurement, SSS and CSI-RS can be used. [3] [11] [12] [13]

As PSS and SSS are included in an SSB, they deserve more study. The detection of the PSS and the SSS is based on correlation calculations. This lead, for example, that the PSS must have low cross-correlation relation with the SSS to avoid fake detections. Also, the SSS must have low auto and cross-correlation between other SSS so that the cell ID is detected correctly. The SSS should also have robustness against a carrier frequency offset (CFO). The PSS and the SSS are built by using a physical cell identity (PCI) and a known sequence. There are 1008 unique identities and those can be divided into two parts: a cell identity (ID) group and a cell ID sector, $N_{\mathrm{ID}}^{(1)} \in \{0,1,\dots,335\}$ and $N_{\mathrm{ID}}^{(2)} \in \{0,1,2\}$, respectively. The PCI is calculated by using

$$N_{\mathrm{ID}}^{\mathrm{cell}} = 3N_{\mathrm{ID}}^{(1)} + N_{\mathrm{ID}}^{(2)}. \quad (1)$$

[1] Only abbreviation of the IMS is opened by using [15].

For finding, for example, a timing location on the transmission window, the UE uses the PBCH as it can carry the timing information. [12] [17] [18]

An M-sequence is used to construct the PSS sequence. The M-sequence is generated by using

$$m = \left(n + 43N_{\mathrm{ID}}^{(2)}\right) \bmod 127, \tag{2}$$

and the PSS sequence is then created by using

$$d_{\mathrm{PSS}}(n) = 1 - 2x(m). \tag{3}$$

The x in the PSS sequence is generated by using

$$x(i+7) = (x(i+4) + x(i)) \bmod 2, \tag{4}$$

where $0 \leq n < 127$ and [$x(6)$ $x(5)$ $x(4)$ $x(3)$ $x(2)$ $x(1)$ $x(0)$]=[1 1 1 0 1 1 0]. [12] [17]

The SSS is created by using

$$d_{\mathrm{SSS}}(n) = \left[1 - 2x_0\left((n + m_0) \bmod 127\right)\right]\left[1 - 2x_1\left((n + m_1) \bmod 127\right)\right], \tag{5}$$

where $0 \leq n < 127$. Equation (5) uses Gold sequences which are generated by using

$$m_0 = 15\left\lfloor \frac{N_{\mathrm{ID}}^{(1)}}{112} \right\rfloor + 5N_{\mathrm{ID}}^{(2)} \tag{6}$$

and

$$m_1 = N_{\mathrm{ID}}^{(1)} \bmod 112. \tag{7}$$

The SSS generator also uses pre-generated x sequences, which are generated by using

$$x_0(i+7) = \left(x_0(i+4) + x_0(i)\right) \bmod 2, \tag{8}$$

and

$$x_1(i+7) = \left(x_1(i+1) + x_1(i)\right) \bmod 2, \tag{9}$$

where [$x_0(6)$ $x_0(5)$ $x_0(4)$ $x_0(3)$ $x_0(2)$ $x_0(1)$ $x_0(0)$]=[0 0 0 0 0 0 1], and [$x_1(6)$ $x_1(5)$ $x_1(4)$ $x_1(3)$ $x_1(2)$ $x_1(1)$ $x_1(0)$]=[0 0 0 0 0 0 1]. [12] [17]

2.3 Numerology and Frame Structure

As NR is designed to support a wide range of the frequencies, it is not feasible to use only one SCS configuration. There are five different configurations in NR which are also called a

numerology. Table 4 shows different numerologies in NR, where μ is a subcarrier space configuration and the subcarrier spacing Δf is calculated by using

$$\Delta f = 2^{\mu} \times 15 \text{ [kHz]}. \quad (10)$$

It is also chosen that 15 kHz is a baseline numerology in 5G NR, just like in LTE. [11] [12]

Table 4. Numerologies in NR

μ	Δf [kHz]
0	15
1	30
2	60
3	120
4	240

In NR, transmissions are designed into frames. Each frame in NR is 10 ms long and the frame duration is calculated by using

$$T_{\mathrm{f}} = \left(\frac{\Delta f_{\max} N_{\mathrm{f}}}{100}\right) \times T_{\mathrm{c}}, \quad (11)$$

where $\Delta f_{\max}$ is the maximum SCS, N_{f} is fast Fourier transform (FFT) size and T_{c} is basic time unit in 5G NR. Then the frame is divided into ten subframes, each 1 ms long and the subframe duration is calculated by using

$$T_{\mathrm{sf}} = \left(\frac{\Delta f_{\max} N_{\mathrm{f}}}{1000}\right) \times T_{\mathrm{c}}. \quad (12)$$

The numbers 100 and 1000 are used to scale the results of equations (11) and (12) to seconds. Also, each subframe is divided into timeslots and each slot includes 14 symbols. Table 5 shows the frame structure in numerical way and Figure 2 visualizes the frame structure where the SCS is 30 kHz (μ=1). [3] [12] [13]

Table 5. Frame structure in numerical way

μ	$N_{\mathrm{subframe}}^{\mathrm{frame},\mu}$	$N_{\mathrm{slot}}^{\mathrm{subframe},\mu}$	$N_{\mathrm{symb}}^{\mathrm{slot}}$	$N_{\mathrm{slot}}^{\mathrm{frame},\mu}$	$N_{\mathrm{symb}}^{\mathrm{frame},\mu}$
0	10	1	14	10	140
1	10	2	14	20	280
2	10	4	14	40	560
3	10	8	14	80	1120
4	10	16	14	160	2240

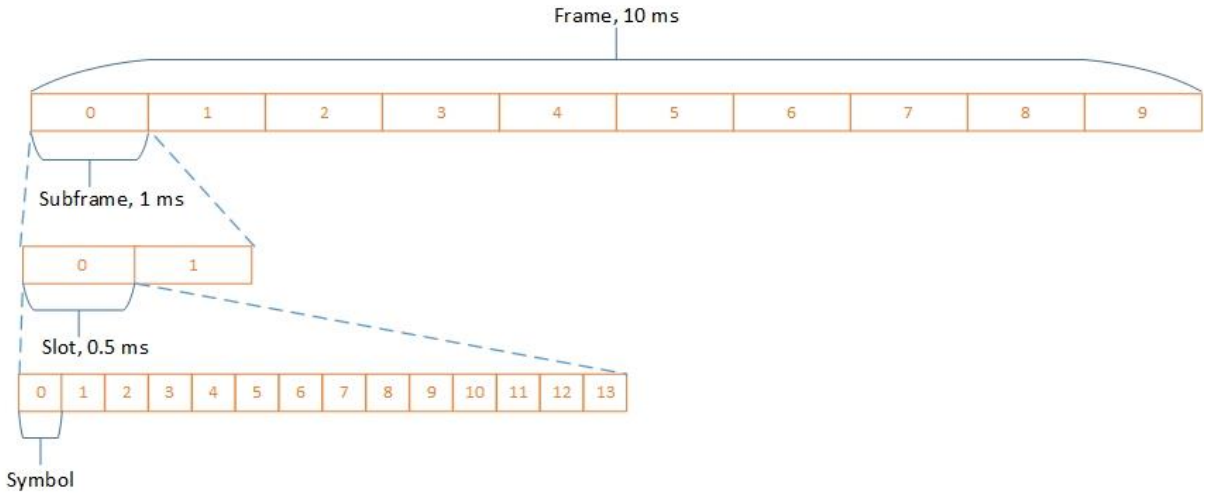

Figure 2. Frame structure when the SCS is 30 kHz.

One key feature in NR is spectrum flexibility. This means that DL and UL can be separated in a time and/or a frequency domain. If the DL and the UL transmissions are separated in the time domain, transmission is called TDD and is seen as a half-duplex transmission. Therefore, in the TDD transmission can happen in one direction at a time. If the transmission is separated in the frequency domain, it is called frequency-division duplex (FDD) and is seen as a full-duplex transmission. In the FDD, the DL and the UL transmissions use different frequencies and therefore transmission can happen in both directions at the same time. However, the FDD transmission can also be a half-duplex if the transmission is separated in the frequency domain but also in the time domain. [3]

In NR, a dynamic TDD is introduced, where the symbols of the slots can be allocated either for DL, UL or for flexible symbols. With the flexible symbols, a user cannot make any assumptions about the direction of the transmission. The flexible symbol can also be used as a guard period time between the DL and the UL symbols. The guard periods are used to ensure that the DL and the UL transmissions does not interfere with each other. The length of the needed guard period depends on a cell size. For example, cell size up to 10.7 km needs two symbols as the guard period, cell size up to 21.4 km needs four symbols as the guard period and cell size up to 32.1 km needs six symbols as the guard period. There are predefined slot formats to tell which symbols are for DL, which are for UL and which are flexible symbols. The slot formats are shown in appendix 1. [3] [19] [20]

2.4 Resource Grid

A transmission can be seen on two different domains: a frequency and a time domain. Linking these two domains together, arise a grid which is called a resource grid. In the grid subcarriers are seen on one axis and OFDM symbols on another axis. The number of the subcarriers in the resource grid are calculated by using

$$N_{\mathrm{grid,x}}^{\mathrm{size},\mu} N_{\mathrm{SC}}^{\mathrm{RB}}, \tag{13}$$

where $N_{\mathrm{grid,x}}^{\mathrm{size},\mu}$ is the size of the resource grid which indicates the number of the resource blocks, where x refers UL, DL or sidelink (SL). $N_{\mathrm{SC}}^{\mathrm{RB}}$ is the number of the subcarriers in a resource block. It is defined, that there are 12 subcarriers in each resource block and up to 275 resource

blocks in a carrier. Each element in the grid is called a resource element and is indicated as $(k, l)_{p,\mu}$, where k is a subcarrier index, l is a OFDM symbol index, p is an antenna port and μ is the numerology. Figure 3 visualizes the resource grid. [12] [15]

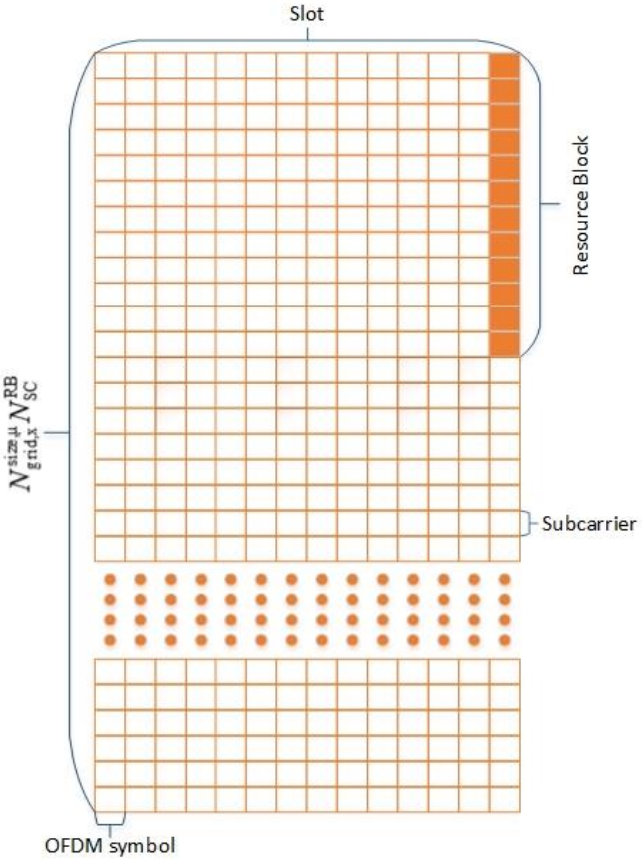

Figure 3. Resource grid.

2.5 Orthogonal Frequency-Division Multiplexing Symbol

NR uses cyclic prefix OFDM (CP-OFDM) in a downlink and in an uplink up to 52.6 GHz frequency. Also, for some uplink scenarios, a discrete Fourier transform spread OFDM (DFTS-OFDM) can be used. There are a couple of reasons for choosing OFDM for NR. Below 30 GHz frequencies there are several crucial key performance indicators (KPIs) for the NR waveform: spectral efficiency, multiple-input multiple-output (MIMO) compatibility, transceiver baseband complexity, robustness to channel time selectivity, robustness to channel frequency selectivity and time localization. CP-OFDM takes these KPIs very well into account and only the robustness to time-selective channels is something where CP-OFDM is not very good nor bad. Also, a cyclic prefix (CP) is used with OFDM symbol as it eliminates intersymbol interference (ISI) between the symbols. Figure 4 illustrates that by taking part from the end of the symbol to the front of the symbol and by designing the CP to be long enough, the ISI is cancelled as the symbols do not override themselves anymore. [11]

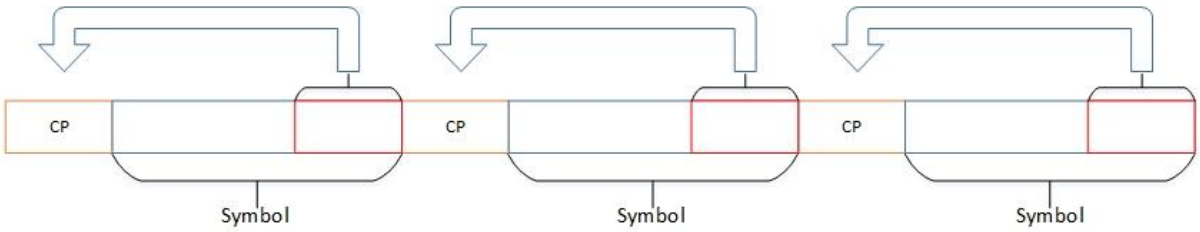

Figure 4. The CP eliminates ISI between symbols.

As mentioned, the time localization can be done very well with the OFDM. For start,

$$T_{\mathrm{c}} = \frac{1}{\Delta f_{\max} N_{\mathrm{f}}} \tag{14}$$

and

$$T_{\mathrm{s}} = \frac{1}{\Delta f_{\mathrm{ref}} N_{\mathrm{f,ref}}} \tag{15}$$

are used to calculate the base time units for NR and LTE, respectively, and Δf_{ref} is the maximum SCS of LTE. $N_{\mathrm{f,ref}}$ is the FFT size of LTE.[2] Then,

$$\kappa = \frac{T_{\mathrm{s}}}{T_{\mathrm{c}}} \tag{16}$$

is used to calculate the ratio of the base units. By using

$$N_{\mathrm{u}}^{\mu} = 2048\kappa \times 2^{-\mu} \tag{17}$$

and

$$N_{\mathrm{CP,l}}^{\mu} = \begin{cases} 512\kappa \times 2^{-\mu} & \text{Extended cyclic prefix} \\ 144\kappa \times 2^{-\mu} + 16\kappa & \text{Normal cyclic prefix}, l = 0 \text{ or } l = 7 \times 2^{\mu} \\ 144\kappa \times 2^{-\mu} & \text{Normal cyclic prefix}, l \neq 0 \text{ or } l \neq 7 \times 2^{\mu} \end{cases} \tag{18}$$

and

$$T_{\mathrm{symb,l}}^{\mu} = \left(N_{\mathrm{u}}^{\mu} + N_{\mathrm{CP,l}}^{\mu}\right) T_{\mathrm{c}}, \tag{19}$$

so the overall CP-OFDM symbol duration can be calculated, where equations (17) and (18) are used to calculate the OFDM useful symbol time and the cyclic prefix length per symbol, respectively, where l is the symbol index. Table 6 shows numerically the CP and the OFDM symbol durations. [3] [11] [12] [21]

[2] [20] is used only to derive meaning for Δf_{ref} and $N_{\mathrm{f,ref}}$.

Table 6. CP and OFDM durations. $\Delta f_{\max} = 480 \times 10^3$ Hz, $\Delta f_{\text{ref}} = 15 \times 10^3$ Hz, $N_{\text{f}} = 4096$ and $N_{\text{f,ref}} = 2048$

μ	Long CP	Short CP	OFDM
0	5.21	4.69	66.67 μs
1	2.86	2.34	33.33 μs

2.6 Detection of Synchronization Block

Synchronization block detection is the critical part of the 5G NR system as it is required, for example, for a cell search. The detection can be divided, for example, into three different stages. The first stage takes places in the time domain while the other stages are done in the frequency domain. The first stage is focused to obtain a symbol time offset (STO) and a CFO. The CFO can be divided into two different offsets: an integer frequency offset (IFO) and a fractional frequency offset (FFO). The IFO can be calculated in the frequency domain while the FFO can be calculated in the time domain. The FFO can then be calculated in two different ways, depending if the CFO is large or not. The CFO is seen as large if, for example, the CFO value, $\epsilon > 1$, otherwise the CFO is seen as small. In the small CFO case, the STO and the FFO can be calculated by using a cross-correlation method. In the case of the large CFO, an autocorrelation method should be used. The second stage of the SSB detection is focused to detect the IFO and the PSS in the frequency domain. The third and final stage of the SSB detection is used to detect the SSS in the frequency domain. [17] [22]

In the cross-correlation method the UE uses known PSS sequences. With the known sequences, the UE can calculate the correlation between the received signal and the known sequence. The cross-correlation is calculated by using

$$C(\theta, i) = \frac{\left|\sum_{k=0}^{N_{\text{FFT}}-1} r(\theta + k) p_{\text{i}}^*(k)\right|}{\sum_{k=0}^{N_{\text{FFT}}-1} |r(\theta + k)|^2} \tag{20}$$

and

$$(\hat{\theta}, \hat{\imath}) = \arg\max_{\theta, i} (C(\theta, i)), \tag{21}$$

where $r(\theta + k)$ is the delayed received signal, $p_{\text{i}}^*(k)$ is the PSS sequence in the time domain for the cell ID sector i and N_{FFT} is a FFT number without CP. The UE can jointly estimate a timing offset $\hat{\theta}$ and a cell ID sector $\hat{\imath}$ and therefore the UE knows the location of the PSS in the time domain. The FFO can be derived by using [17]

$$\hat{\epsilon}_{\text{FFO}} = \frac{1}{\pi} \angle \left(\left[\sum_{k=0}^{\frac{N_{\text{FFT}}}{2}-1} r(\hat{\theta} + k) p_{\hat{\imath}}^*(k) \right]^* \times \left[\sum_{k=\frac{N_{\text{FFT}}}{2}}^{N_{\text{FFT}}-1} r(\hat{\theta} + k) p_{\hat{\imath}}^*(k) \right] \right). \tag{22}$$

In the auto-correlation method, the received signal is correlated with the cyclic prefix part. The autocorrelation method can be used to calculate the FFO if the CFO is large. Equation

$$\gamma(\theta) = \sum_{k=\theta}^{\theta+L-1} r(k) r^*(k + N_{\text{FFT}}) \tag{23}$$

represents a correlation calculation and

$$\alpha(\theta) = \sum_{k=\theta}^{\theta+L-1} |r(k)|^2 + |r^*(k+N_{\mathrm{FFT}})|^2 \tag{24}$$

represents the energy part of the estimation. By adding those two equations into

$$\hat{\theta} = \max_{\theta} \big(2|\gamma(\theta)| - \rho \angle \alpha(\theta)\big), \tag{25}$$

the timing estimation can be calculated. In equation (25), ρ is the magnitude of the correlation coefficient and is calculated by using

$$\rho = \frac{\sigma_s^2}{\sigma_s^2 + \sigma_N^2}, \tag{26}$$

where σ_s^2 and σ_N^2 represents a signal and a noise power, respectively. Then by using

$$\hat{\epsilon} = -\frac{1}{2\pi} \angle \left(\gamma\left(\hat{\theta}\right)\right), \tag{27}$$

the FFO is estimated. The autocorrelation method can be improved by averaging out the results over multiple symbols. When comparing the autocorrelation method to the cross-correlation method, the cell ID sector cannot be derived but it results the more accurate estimations of the FFO. [17]

The second stage is focused to calculate the IFO and detect the PSS in the frequency domain. As the cell ID sector is used to construct the PSS, it means that there could be three different PSS signals. In the following equations the predefined PSS sequence per a cell ID sector is seen as P_{w}, where $\mathrm{w} \in \{0,1,2\}$ represents the cell ID sector. The PSS is spread into 127 subcarriers. Subcarrier index is shown as k in the equations and so $Y_1(k)$ is the received frequency domain signal in kth subcarrier. Now it is assumed that the STO is evaluated correctly, and the time location of the PSS is detected. The correlation of the PSS is calculated by inserting differential

$$\bar{Y}_1(k) = Y_1(k) Y_1^*(k-1) \tag{28}$$

and

$$D_{\mathrm{w}}(k) = P_{\mathrm{w}}(k) P_{\mathrm{w}}^*(k-1) \tag{29}$$

to

$$\Phi_{\mathrm{PSS}}(m,w) = \sum_{k\epsilon\mathbb{D}} \bar{Y}_1(k+m) D_{\mathrm{w}}^*(k), \tag{30}$$

where $m \in \{-G, G+1, \dots, G\}$ is representing the assumed value of the normalized IFO and $\mathbb{D} = \{k | 57 \le k \le 182\}$. To estimating the IFO and the cell ID sector

$$(\hat{\epsilon}_{\mathrm{IFO}}, \hat{u}) = \arg\max_{\mathrm{m,w}} \Re\{\Phi_{\mathrm{PSS}}(m, w)\}, \tag{31}$$

is used, where $\hat{\epsilon}_{\mathrm{IFO}}$ represent the estimated IFO and $\hat{u}$ representing the estimated cell ID sector. [22]

At the third stage, the SS signal is detected in the frequency domain. It is performed either a coherently or a noncoherently. In the coherent correlation method, the UE uses some information which has been detected from the PSS detection process. The coherent detection uses

$$\Phi_{\mathrm{SSS}}(c) = \sum_{k=56}^{182} \left(Y_{\mathrm{l}}(k + \hat{\epsilon}_{\mathrm{IFO}}) P_{\hat{\mathrm{u}}}^{*}(k)\right)^{*} Y_{\mathrm{l}+2}\left(k + \hat{\theta}\right) S_{\mathrm{c}}^{*}(k), \tag{32}$$

where k is the subcarrier index, $Y_{\mathrm{l}}\left(k + \hat{\theta}\right) P_{\hat{\theta}}^{*}(k)$ is the PSS-recovered signal, $Y_{\mathrm{l}+2}(k)$ is the received SSS symbol, $S_{\mathrm{c}}(k)$ is the predefined SSS sequence per cell id group and $c = \{0, 1, 2, \ldots, 335\}$. The noncoherent correlation method is calculated by using

$$\Phi_{\mathrm{SSS}}(c) = \sum_{k=56}^{182} Y_{\mathrm{l}+2}\left(k + \hat{\theta}\right) Y_{\mathrm{l}+2}^{*}\left(k + \hat{\theta} - 1\right) S_{\mathrm{c}}^{*}(k) S_{\mathrm{c}}(k - 1). \tag{33}$$

After calculating the correlations by either method, the SSS can be estimated by taking the maximum correlation

$$\hat{g}_{\mathrm{SSS}} = \arg\max_{\mathrm{c}} |\Phi_{\mathrm{SSS}}(c)|. \tag{34}$$

Now the SSS is detected for the cell measurements and the cell id can be calculated by using (1), where $N_{\mathrm{ID}}^{(1)} = \hat{u}$ and $N_{\mathrm{ID}}^{(2)} = \hat{g}$. [22]

3 CELL MEASUREMENT IN NEW RADIO

This chapter introduces the overview of the cell measurement procedure but also cell measurement resources, parameters and requirements in NR. The chapter focuses on giving basic information which can be used in NR-U with some differences. The differences between NR and NR-U in cell measurements are covered in Chapter 4.

3.1 Overview of Cell Measurements

Cell measurements in 5G NR are based on beams. A beam is created from a base station by transmitting a reference signal. On the UE side, SSB and CSI-RS are used for the cell measurements but in 5G NR, mobility measurements are usually performed by using the SSB. A group of the SSBs is called SSB burst set and the burst set is transmitted periodically. Figure 5 visualizes the relation between the SSB burst set and the beams: beam 1 corresponds to SSB 1, beam 2 to SSB 2 and so on. From the beam, the UE should be able to measure RSRP, RSRQ and SINR in both licensed and unlicensed spectrum [15]. By using the results of the measurements, the network could control, for example, the mobility of the devices. A measurement is one-shot measurement and to make accurate decisions, the UE must measure beams multiple times, for example, over a hundred milliseconds, and average the results over the period of the time. [3]

Figure 5. SSB burst sets from base station at the time domain.

There are three different states for UE: RRC_IDLE, RRC_INACTIVE and RRC_CONNECTED [13]. At idle and inactive state, mobility is handled by the device. To be able to perform, for example, cell search or cell reselection, RSRP and RSRQ must be measured by the UE and the measurements have to be performed at least two times. At connected state, the mobility is handled by the network and measurements are performed continuously. In all states, the UE should be able to measure the RSRP and the RSRQ but the SINR is only measured at the connected state. [3] [7] [23]

From the protocol perspective the measurement procedure takes place at Layer 1 (L1) and Layer 3 (L3). First, the UE measures RSRP, RSRQ and SINR from multiple beams. Those results are given to L1 for filtering which average the results. The filtering is UE specific and is therefore not standardized procedure. From the filtered results, the UE derives beam and cell qualities which is a standardized procedure. A report is sent from the UE to the network, and the report can include, for example, RSRP. Figure 6 visualizes the measurement procedure from the beam power measurements to the report evaluation. [3] [13]

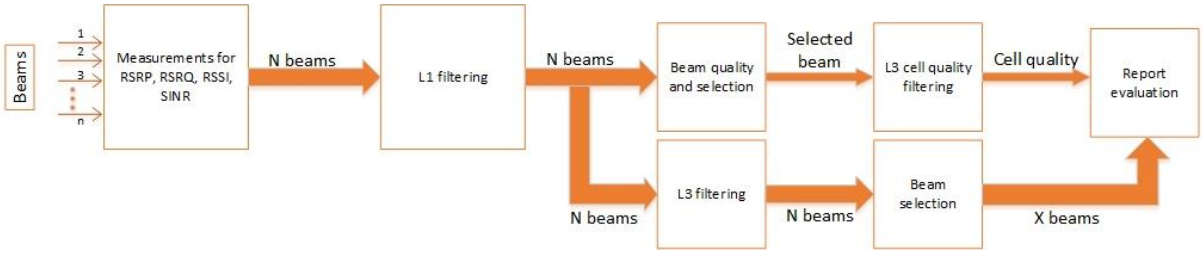

Figure 6. Measurement process at L1 and L3.

3.2 Synchronization Signal Block

An SSB, which is also known as a SS/PBCH block, contains PSS, SSS, PBCH and DM-RS for the PBCH. In time domain, the SSB occupies 4 OFDM symbols and on frequency domain up to 240 subcarriers. The first symbol of the SSB is used for the PSS and it uses subcarrier indices 56—182. All other subcarriers are set to zero. The second and the fourth OFDM symbols are used by the PBCH and the DM-RS and they occupy all 240 subcarriers. The DM-RS takes every $0+\nu, 4+\nu, \ldots, 236+\nu$ subcarriers, where the quantity ν is calculated by using

$$\nu = N_{\mathrm{ID}}^{\mathrm{cell}} \bmod(4). \tag{35}$$

Other subcarriers which are left from the DM-RS, are used for the PBCH. [12]

Third OFDM symbol is for the SSS and it takes same subcarrier indices as the PSS. However, the third OFDM symbol differs a bit from the first one as now the PBCH uses subcarriers 0 to 47 and 192 to 239. The DM-RS for the PBCH uses subcarriers $0+\nu, 4+\nu, \ldots, 44+\nu$ and $192+\nu, 196+\nu, \ldots, 236+\nu$. Figure 7 illustrates the SSB design in the time and the frequency domain. [12]

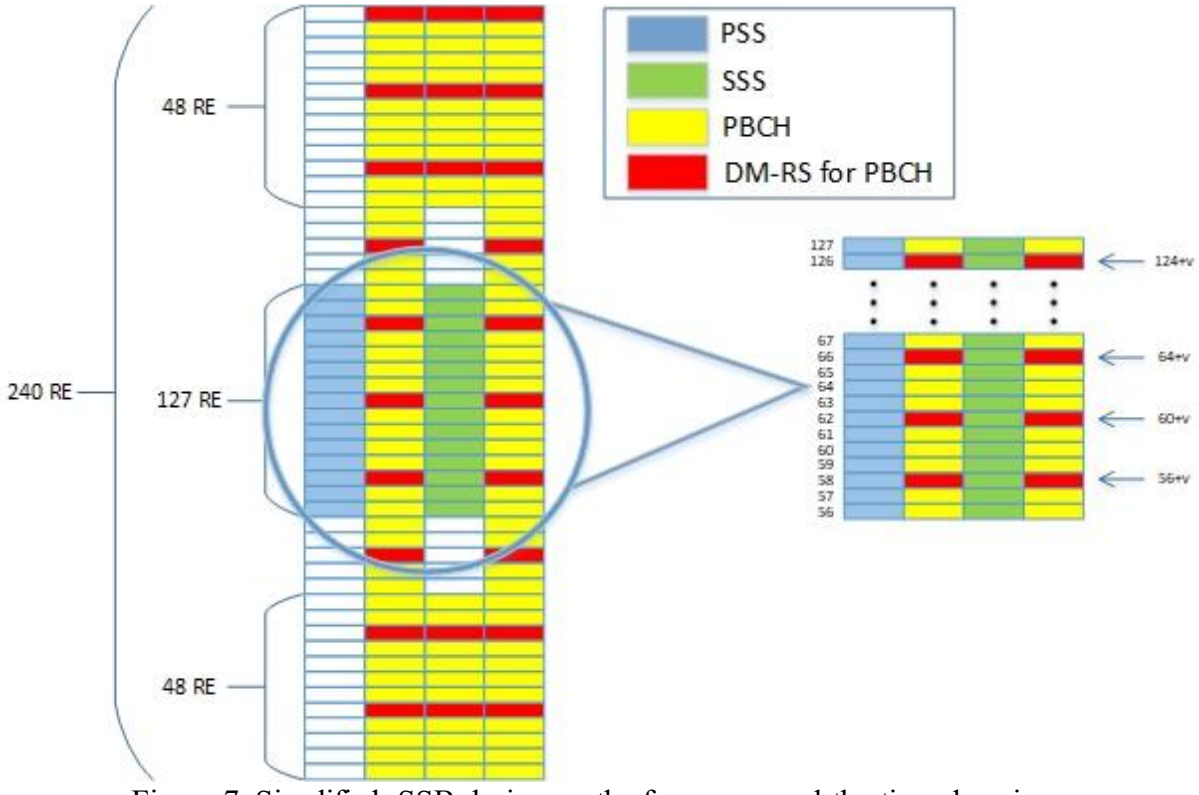

Figure 7. Simplified SSB design on the frequency and the time domain.

In NR, the SSB transmissions are considered in half-frames and in the half-frame it is possible to transmit multiple SSBs if they are transmitted from different beams. As the SSB transmission in NR is a periodic, the SSB locations in the time domain are kind of locked. Once the UE has located the SSB, it should be transmitted again after the certain period of time. There are five different classes for candidate SSB locations, which are identified by the subcarrier spacing and the frequency. The SSB can be located at any of those candidate locations, but the certain SSB should always be in the same candidate location from time to time so that the periodic requirement is fulfilled. The classes for the candidate locations are named from Case A to Case E. Those cases can also be divided into two different groups as 15 kHz and 30 kHz subcarrier spacing belongs to FR1 region and 120 kHz and 240 kHz subcarrier spacing belongs to Frequency Range 2 (FR2) region. It is notable that 60 kHz subcarrier spacing, and extended CP are not used with the SSB transmission. As the unlicensed frequencies are within FR1 region, Table 7 shows different cases and candidate locations for FR1 frequencies. Starting indices at Table 7 are the first OFDM symbols of the SSB. As Table 7 shows, the maximum number of SSB locations could be either four or eight, depending on the used frequency. In 5G NR, all locations can be filled so the maximum supported beam number can be either four or eight, depending again, on the used frequency. Figure 8 visualizes the SSB locations when the base station transmits four different SSBs. [13] [20]

Table 7. The starting indices of the SSB locations

Cases	Equations and exceptions	Starting indices
Case A: SCS = 15 kHz	$\{2, 8\} + 14 \times n$	
	if <=3 GHz: $n = 0,1$	2, 8, 16, 22
	if > 3 GHz: $n = 0,1,2,3$	2,8,16,22,30,36,44,50
Case B: SCS = 30 kHz	$\{4, 8, 16, 20\} + 28 \times n$	
	if <= 3 GHz: $n = 0$	4, 8, 16, 20
	if > 3 GHz: $n = 0,1$	4,8,16,20,32,36,44,48
Case C: SCS = 30 kHz	$\{2, 8\} + 14 \times n$	
	if < 1.88 GHz or <= 3GHz: $n = 0,1$	2, 8, 16, 22
	if >= 1.88 GHz or > 3 Ghz: $n = 0,1,2,3$	2,8,16,22,30,36,44,50

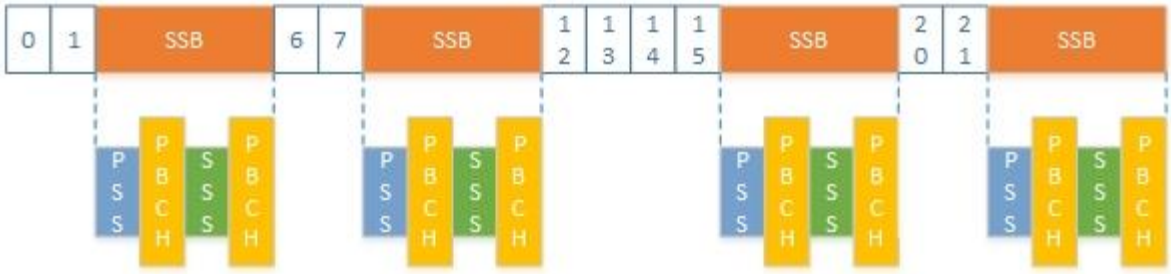

Figure 8. SSBs locations at the time domain.

3.3 Parameters of Cell Measurements

UE should be able to measure RSRP, RSRQ and SINR by using a SSB or an CSI-RS. This thesis is focused only to the SSB measurements and therefore following parameters are considered only in view of the SSB.

3.3.1 Reference Signal Received Power

In synchronization signal based RSRP measurement, the power of the resource elements of the secondary synchronization signal is measured and linearly averaged over the resource elements. The RSRP is measured in watts and a measurement window is limited to a SS/PBCH Block Measurement Time Configuration (SMTC) window duration. In the FR1 region, a reference point for the RSRP is the antenna connector of the UE. The RSRP could be measured in all states and in both intra and inter-frequency measurements. [23]

3.3.2 Reference Signal Received Quality

A synchronization signal based RSRQ is indicating quality of the received signal and it is calculated by using

$$\frac{N \times RSRP}{RSSI}, \tag{36}$$

where N is the number of the measured resource blocks in a carrier. RSSI comes from received signal strength indicator (RSSI) which has been calculated by averaging the total power of the certain amount of the OFDM symbols including all sources, interferences and noise. In cell selection, a measurement time is not considered, but in other measurement situations, the RSSI measurement time is limited within the SMTC window. In the FR1, a reference point for the RSRQ measurement is the antenna connector of the UE. The RSRQ is measured in all states and in both inter and intra-frequency. [23]

3.3.3 Reference Signal-to-Noise-plus-Interference Ratio

A synchronization signal based SINR is calculated by dividing the RSRP by the linear average of noise and interference. The time window for the measurement is limited within the SMTC window duration. In the FR1, a reference point for the SINR is the antenna connector of the UE. The SINR is only measured at RRC_CONNECTED state. [23]

3.4 Requirements

As described earlier, the UE should be able to measure RSRP, RSRQ and SINR. In RRC_CONNECTED state, the UE could either measure intra or inter-frequencies. Measurement is an intra-frequency measurement if the centre frequency of the SSB at the serving cell is the same as the centre frequency of the SSB at a neighbour cell. Also, the subcarrier spacing between the SSBs should be the same. If one of two requirements is not fulfilled, measurement can be seen as an inter-frequency measurement. In the intra-frequency measurements, the UE should have capability for one to two different SMTCs per a carrier and in the inter-frequency measurements only one SMTC is required. The SMTC provides information about periodicity, duration and offset of the measurement window. The time frame

for the periodicity is from five ms to 160 ms and the time frame for the duration is from one ms to five ms. Figure 9 visualizes the terms of the duration and the periodicity [7] [15]

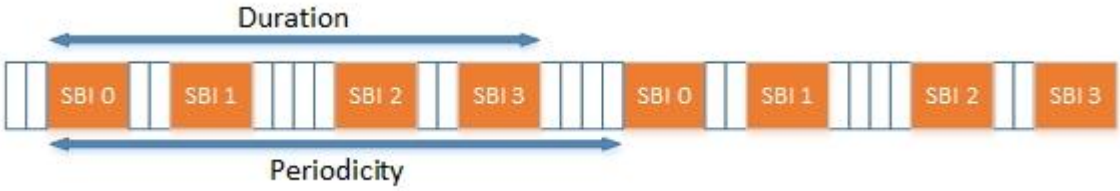

Figure 9. Visualization of the SSB duration and periodicity.

In the intra-frequency measurements at the FR1 spectrum, the UE should be able to measure up to 8 cells and up to 14 SSBs with different SSB index and PCI at the same time. In the inter-frequency measurements at the FR1 spectrum, the UE should be able to measure up to 4 cells and 7 SSBs with different SSB index and PCI at the same time. [7]

Absolute RSRP accuracy requirements for the UE at intra and inter-frequency measurements can vary ± 4.5 dB or ± 8 dB and total received power density (Io) range is from -121 dBm to -50 dBm, depending on the operating band and the SCS. Absolute RSRQ requirements for the UE at intra and inter-frequency measurements can vary ± 2.5 dB or ± 3.5 dB and the Io range is from -121 dBm to -50 dBm, depending on the operating bands and the SCS. Absolute SINR requirements for the UE at intra and inter-frequency measurements can vary ± 3.0 dB or ± 3.5 dB and the Io range is -121 dBm to -50 dBm, depending on the operating bands and the SCS. [7]

4 CELL MEASUREMENT IN UNLICENSED SPECTRUM

This chapter introduces differences between NR and NR-U in cell measurement. The chapter also introduces the purpose of the QCL expansion in NR-U. Also, the used spectrum and channel access mechanism are presented as those topics are very close related on the cell measurement.

4.1 Spectrum

In NR-U there are basically two frequency groups: a low and a high-frequency groups. The frequencies from 410 MHz to 7125 MHz belong to the low-frequency group and the frequencies from 24250 MHz to 52600 MHz belong to the high-frequency group [14]. 3GPP is targeting NR-U for the bands of Unlicensed National Information Infrastructure (UNII) frequencies. The UNII frequency range starts from 5.15 GHz and ends at 7.125 GHz. The UNII spectrum is then divided into ten different categories, named UNII-1 to UNII-8, where UNII-2 is further split into three different categories, UNII-2A, UNII-2B and UNII-2C. The use of the UNII-2B and the UNII-4 bands for NR-U is forbidden. The differences between the UNII bands are maximum transmit power, EIRP, applicability for indoor and/or outdoor operations and requirement for DFS. [24]

NR-U can support up to 100 MHz bandwidth without carrier aggregation. However, it is agreed, that by default at 5 GHz spectrum, NR-U uses 20 MHz bandwidth for LBT to enable a fair coexistence with other systems. [25]

4.2 Downlink Channel Access

NR-U supports two different channel access mechanisms: a dynamic channel access and a semi-static channel access. In the dynamic channel access mechanism, the transmitter listens to the channel if it is busy or idle. If the channel is in idle state, after a random back-off the transmitter may start transmission if possible. The dynamic channel access mechanism follows the same principles as Wi-Fi and is mandatory, for example, in Europe and Japan. The access mechanism is based on LBT which have four different categories. In categories 1 and 2, a device can send data after a fixed time interval and in categories 3 and 4 a device can send data after a fixed time interval and the random number of time slots. Category 4 is similar to a technology which is used in Wi-Fi. The semi-static channel access mechanism does not use the random back-off but instead the transmitter starts a transmission at the certain point of the time. A period when the transmitter can use the channel is called channel occupancy time (COT). Within the period, the channel can be used either for downlink or uplink transmission or for both downlink and uplink transmission which is called COT sharing. Transmissions are seen as bursts, where gaps between transmissions are not greater than 16 µs. If the gap between two transmission is greater than 16 µs, then the transmissions are in different bursts. [3] [4] [8]

A sensing measurement happens within a sensing slot T_{sl} which length is 9 µs. The channel is in idle state if the base station or the UE is sensing less power than an energy detection threshold X_{Tresh} and the base station or the UE is sensing that power for at least 4 µs. Otherwise, the channel is considered busy during the slot. X_{Tresh} is configured to the UE and it can be less or equal than the value of the maximum energy detection threshold $X_{\mathrm{Tresh\_max}}$ which can be anything between -85 dBm to -52 dBm. However, with 5 GHz band and 20 MHz carrier, the $X_{\mathrm{Tresh\_max}}$ is set to -72 dBm. The choice of the $X_{\mathrm{Tresh\_max}}$ is made as Wi-Fi uses -62 dBm value if Wi-Fi preamble is not detected and -82 dBm otherwise. If 5G NR is the only technology

using the wireless medium, the $X_{\text{Tresh\_max}}$ is then set to -62 dBm if no other requirement requires otherwise. [3] [8] [15]

There are two mainly used dynamic channel access procedures for the DL: Type 1 and Type 2. Type 1 follows the LBT category 4 and procedure is initiated either by an eNodeB (eNB), a gNodeB (gNB) or a UE. Procedure starts by sensing the channel to be idle for T_{d} duration. T_{d} is built by duration $T_{\text{fd}} = 16\ \mu\text{s}$ and m_{p} sensing slots so that

$$T_{\text{d}} = T_{\text{fd}} + m_{\text{p}} \times T_{\text{sl}}. \tag{37}$$

The number of the sensing slots m_{p} depends on a channel access priority class (CAPC) p and is shown in Table 8.

Table 8. Channel access priority classes

p	m_{p}	$CW_{\text{min,p}}$	$CW_{\text{max,p}}$	$T_{\text{mcot,p}}$
1	1	3	7	2 ms
2	1	7	15	3 ms
3	3	15	63	8 or 10 ms
4	7	15	1023	8 or 10 ms

After sensing the channel to be idle, eNB/gNB initializes a random backoff counter N which is a random uniformly distributed number between 0 and CW_{p}. The number of the CW_{p} depends on p. The bounds of the CW_{p} are shown in Table 8 and the CW_{p} is the number chosen between $CW_{\text{min,p}}$ and $CW_{\text{max,p}}$. After the initialization, the procedure loop starts and is visualized in Figure 10.

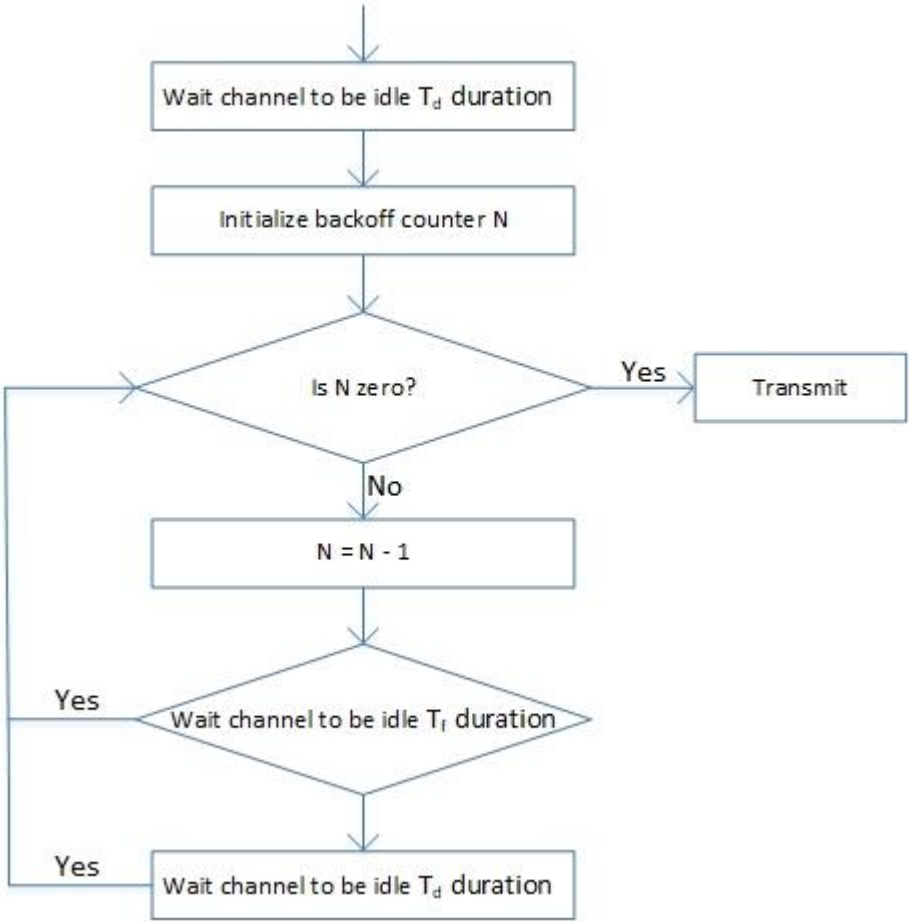

Figure 10. Type 1 channel access procedures.

After the procedure is finished successfully, the initiator of the procedure can use the channel during COT and the initiator can perform one or multiple transmissions on the channel. Maximum COT (MCOT) is referred as $T_{\mathrm{mcot,p}}$ and it depends on the priority p. Table 8 shows different MCOT lengths. [3] [8]

It is also possible to share COT. By sharing, it is possible to use the channel for uplink and downlink transmissions. Sharing the COT is called COT sharing and depending on the gap between the transmission bursts within COT, different channel access mechanisms are used. These mechanisms are simplified compared to Type 1, and therefore Type 1 can be used only for the initial access.

For COT sharing, Type 2 is used and is divided into three different category, Type A to C. The main differences between Type 2A, 2B and 2C is that Type 2A and 2B have the channel sensing procedure which Type 2C does not have. Type 2A, and 2B are also a bit similar to Type 1 but without the random back-off process. Type 2A can be seen as LBT category 2 and is used if the gap between transmission bursts is equal or longer than 25 µs. In that case, the transmission can be performed after the channel is sensed to be idle for at least $T_{\mathrm{short\ dl}} = 25$ µs. Type 2A can also be used for broadcast transmissions, for example, SSB transmissions if standalone NR-U is used. If the gap between transmission bursts is equal to 16 µs, Type 2B is used. In type 2B, the transmission can be performed after the channel is sensed to be idle during $T_{\mathrm{f}} = 16$ µs. In Type 2C, the initiator does not sense the channel before the transmission, but the transmission can take at the most 584 µs. However, to use Type 2C, the transmission must start within 16 µs after previous transmission so that the sensing is not needed. [3] [8]

The semi-static channel access can be used if it can be guaranteed that no other RATs are using the wireless medium. In this access mechanism, the COT occurs periodically with interval T_x which can be from 1 ms to 10 ms long. To enable fair coexistence with other transmitters, the COT must end before at least 5% of the T_x and at least 100 µs before the next COT. The transmitter must also sense the channel to be idle for at least 9 µs before it can start the transmission. If the transmitter is sensing the channel to be busy, it must wait until the next transmission window occurs. Figure 11 visualizes the semi-static channel access mechanism. [3]

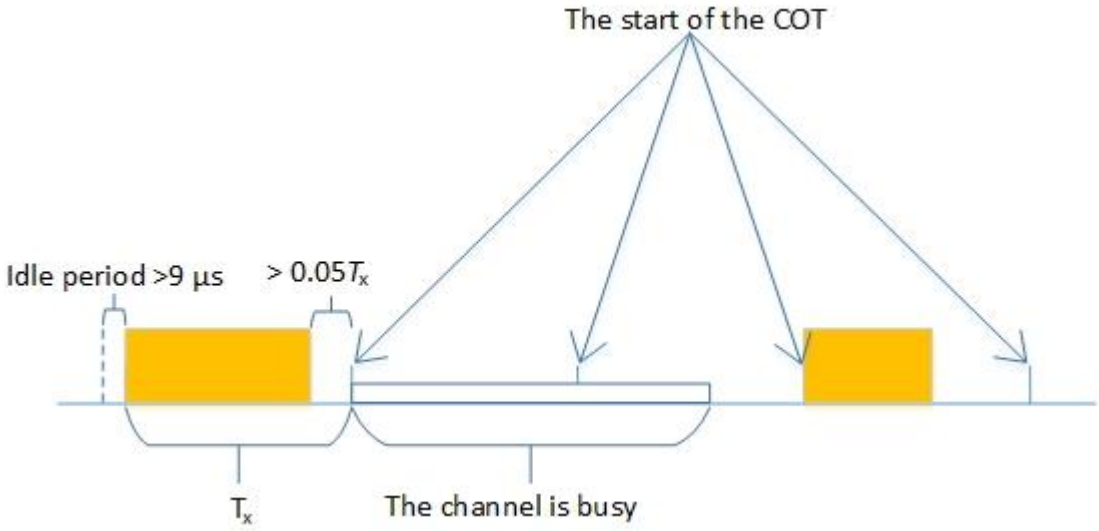

Figure 11. Semi-static channel access mechanism.

4.3 Quasi Co-Location

There are four different types of the QCL, typeA to typeD. All the types tell something about the properties a channel can have. For example, in typeA, a device should consider the effects of doppler shift, doppler spread, average delay and delay spread. Table 9 shows all the types of the QCL. Two signals can be seen as Quasi Co-Located if they have been transmitted from different antennas, but their spaces are very close to each other so they can share the same large-scale properties, as for example the doppler spread or the delay. [11] [26]

Table 9. The types of the QCL

typeA	Doppler shift, Doppler spread, average delay, delay spread
typeB	Doppler shift, Doppler spread
typeC	Doppler shift, average delay
typeD	Spatial Rx parameter

The SSB QCL assumption differs between NR and NR-U. The difference is that in 5G NR, the SSB QCL assumption is valid only for the SSBs with the same block index on the same centre frequency location. It is not possible to have the QCL assumption between other SSBs. This means that the SSBs are quasi co-located in NR only when transmitted from the same beam. In NR-U this assumption differs a bit as when the UE is using the unlicensed spectrum, it can assume that the SSBs are Quasi Co-Located if the SSBs are transmitted from the serving cell and within a same discovery burst transmission window or across discovery burst

transmission windows. Within the discovery burst or bursts, the location of the SSB is derived by using

$$N_{\mathrm{DM-RS}}^{\mathrm{PBCH}} \mathrm{mod}\left(N_{\mathrm{SSB}}^{\mathrm{QCL}}\right), \tag{38}$$

where $N_{\mathrm{DM-RS}}^{\mathrm{PBCH}}$ is the index of DM-RS sequence which is transmitted with the PBCH. $N_{\mathrm{SSB}}^{\mathrm{QCL}}$ is also the upper boundary of the number of transmitted SSBs and is provided to the UE by the network. The value of the $N_{\mathrm{SSB}}^{\mathrm{QCL}}$ can be either one, two, four or eight. Table 10 shows the number of possible locations per SSB in a half-frame with the different values of the $N_{\mathrm{SSB}}^{\mathrm{QCL}}$ and with different subcarrier spacings.

Table 10. The number of the candidate locations per SSB with 15 kHz and 30 kHz SCS.

$N_{\mathrm{SSB}}^{\mathrm{QCL}}$	Candidate locations per SSB with 15 kHz SCS	Candidate locations per SSB with 30 kHz SCS
1	10	20
2	5	10
4	2 to 3	5
8	1 to 2	2 to 3

The QCL expansion makes time shifting possible for the SSB and the number of the candidate locations is increased.

Figure 12 visualizes the effect of the $N_{\mathrm{SSB}}^{\mathrm{QCL}}$ when 15 kHz SCS is used and the value of $N_{\mathrm{SSB}}^{\mathrm{QCL}}$ is two. The arrow in the figure points to the possible locations for the SSB with index 0. In both NR and NR-U cases, the SSBs are Quasi Co-Located in respect to average gain, typeA and typeD, if possible. [3] [12] [15] [20]

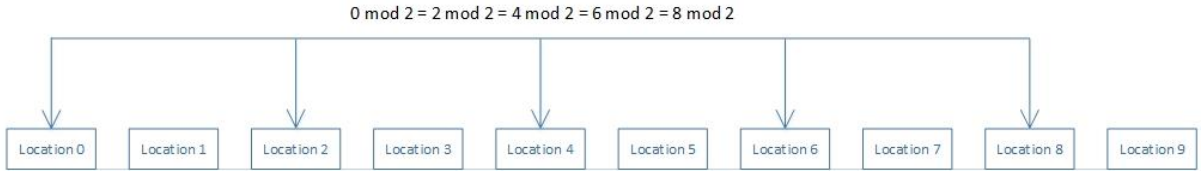

Figure 12. QCL relations when $N_{\mathrm{SSB}}^{\mathrm{QCL}} = 2$. Possible locations for SSB 0.

4.4 Synchronization Signal Block

To operate in the unlicensed spectrum, LBT must be used. However, the LBT has impacts to SSB transmission, which is periodical in NR. Because of the LBT, the periodicity of the SSB transmission does not apply anymore in NR-U as a base station cannot control a channel. To resolve challenges due to the LBT, a discovery burst and the expanded QCL assumption of the SSB are used. The discovery burst is defined as a block, which include at least one SSB but also a control resource set (CORESET) for PDCCH and PDSCH with SIB1. The block may also include non-zero power CSI-RS. It is sent within the discovery burst transmission window which could be from 0.5 ms to 5 ms long. Figure 13 visualizes a discovery burst design.

Figure 13. NR-U discovery burst structure.

TS 38.213 defines that the maximum number of SSB locations is increased from eight to ten when SCS is 15 kHz and eight to 20, when SCS is 30 kHz. However, the maximum number of transmitted SSBs stays as eight which leads to empty candidate locations on the time domain. This differs a bit from NR, where the maximum number of the transmitted SSBs is equal to the maximum number of candidate locations. Table 11 shows the all possible candidate locations of half frame in NR-U and Figure 14 visualizes the candidate locations of SSB transmissions in NR-U. [3] [8] [15] [20]

Table 11. The starting indices of the SSB locations

Cases	Equations and exceptions	Starting indices
Case A: SCS = 15 kHz	$\{2,8\} + 14 \times n$	2,8,16,22,30, 36,44,50,58,64
	$n = 0,1,2,3,4$	
Case B: SCS = 30 kHz	$\{2,8\} + 14 \times n$	2,8,16,22,30, 36,44,50,58,64, 72,78,86,92,100, 106,114,120,128,134
	$n = 0,1,2,3,4,5,6,7,8,9$	

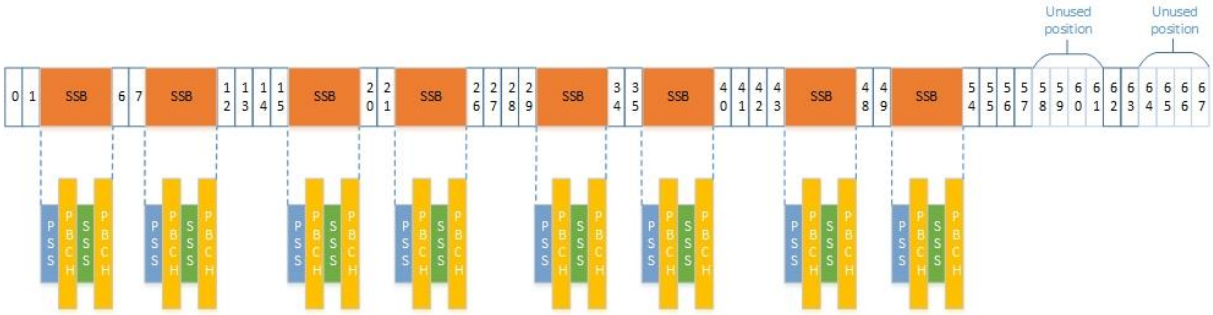

Figure 14. An example of candidate locations of the SSBs in NR-U.

Another improvement in NR-U, is the possibility to the time shift of the SSB within the transmission window. Shifting can be done either by waiting until the channel is free and then send the SSBs or by wrapping the SSBs which are intended to be sent during the LBT to the end of the burst. Figure 15 visualizes both methods. [25]

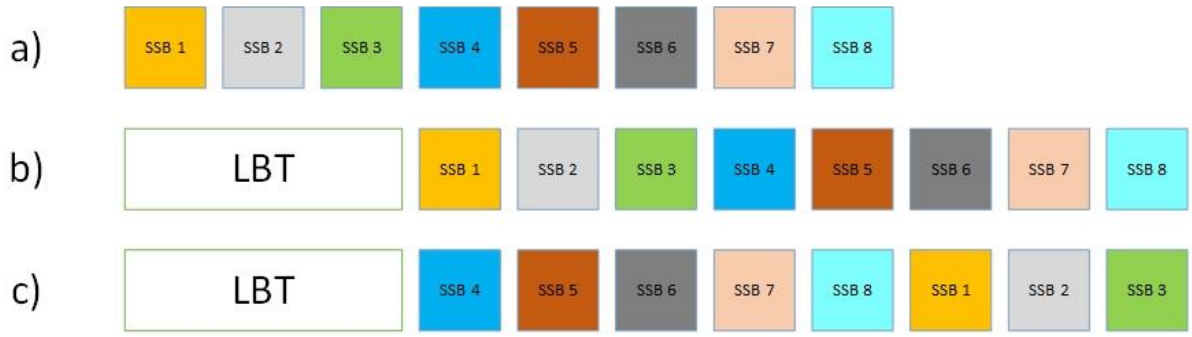

Figure 15. SSB transmission methods in NR-U. a) correspond to intended transmission b) correspond to shifted transmission and c) correspond to wrapped transmission.

5 IMPLEMENTATION

In this chapter, the implementation part of the thesis is introduced. First, a short introduction for the overall design of cell measurement is presented and then a view for the FW part. After the overview of the implementation, the main challenges are shown and how the challenges are solved. Finally, the test environment and the configurations are introduced.

5.1 Overview

The part of cell measurement is performed in the FW. The process starts when higher layer sends a request to a measurement unit (MU) to capture data. After that the higher layer triggers the FW to wait for data to be captured and when it is available, the FW performs calculations. It is notable, that the FW part of the cell measurement design is focusing only to one-shot measurements while other layers handle multiple measurements for the decisions. Figure 16 visualizes the process.

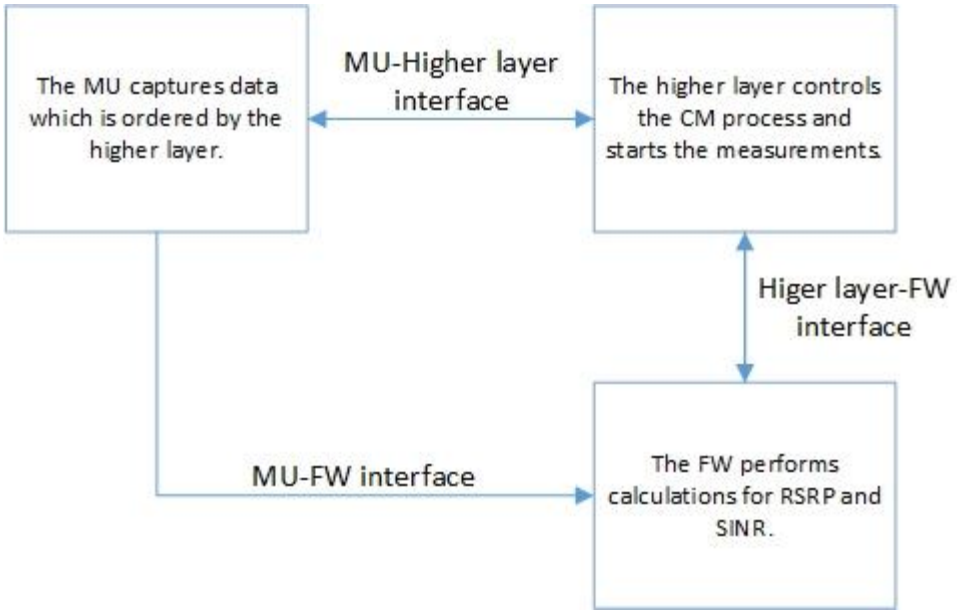

Figure 16. Cell measurement process.

When the FW receives data from the MU, it starts to process it. First, the FW identifies a candidate location to see if an SSB could be on that location. After the location is identified, the FW sets the beam of the candidate location into a queue and continues with the next candidate location. After all locations are identified and the beams of the candidate locations are set into the queue, the FW starts the process to calculate RSRP and SINR. With the SINR, the FW can decide the true locations of the SSBs. The results of the cell measurements are per a beam and it include information about the location of the beam on the time domain and the power of the SSS. The results are then sent to the higher layer for its own processes, for example, for cell reselection. Figure 17 visualizes the process from the FW point of view.

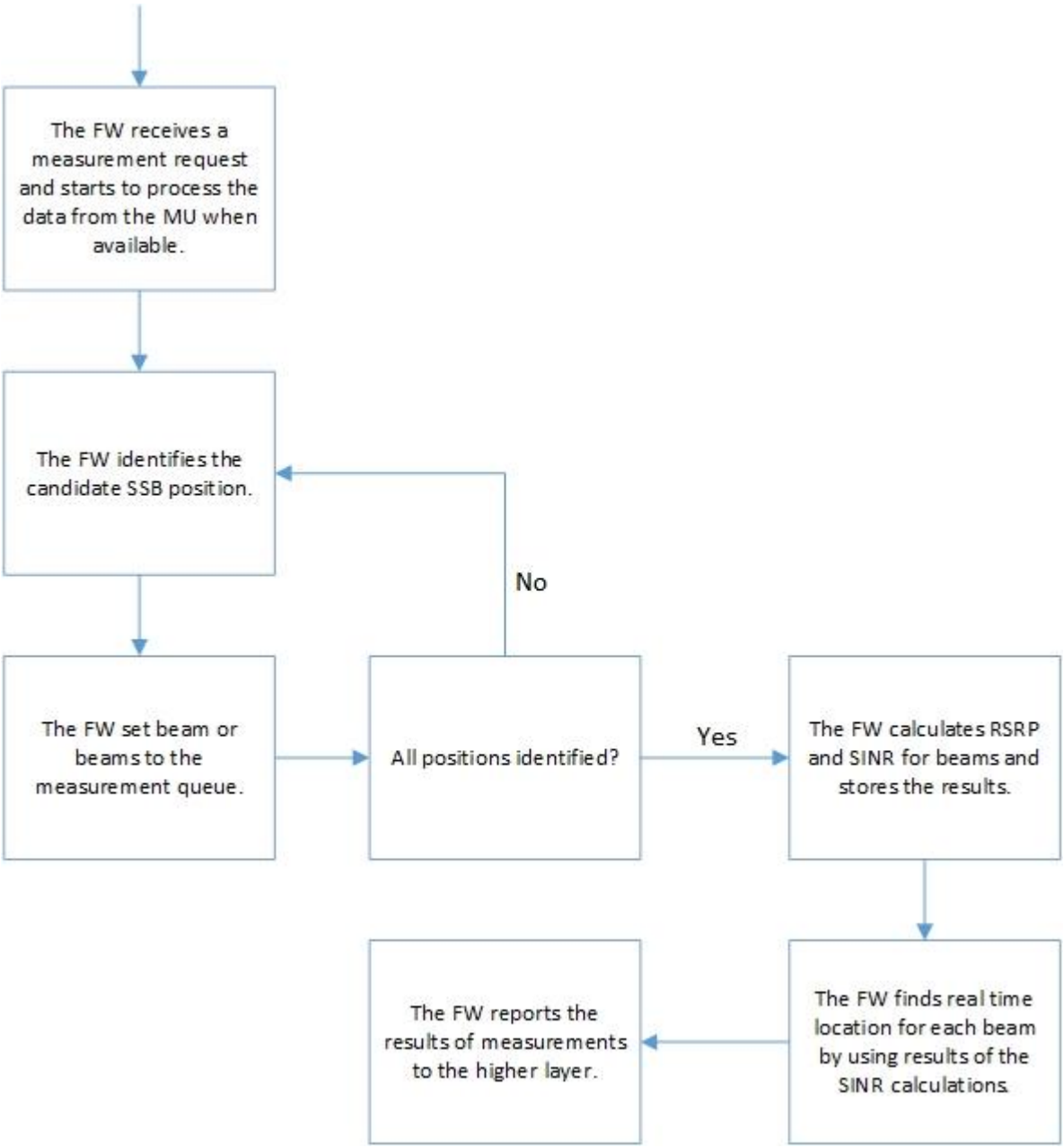

Figure 17. The FW process for cell measurements.

5.2 Challenges and Solution

As introduced earlier, SSBs are Quasi co-located within discovery transmission windows. This means that the SSBs can be time shifted to different candidate locations according to Table 11. The locations for different SSBs are calculated by using (38), where $N_{\mathrm{SSB}}^{\mathrm{QCL}}$ refers to the maximum number of the SSBs in the discovery burst. Figure 18 shows candidate locations for SSB 1 when SCS is 15 kHz and the value of $N_{\mathrm{SSB}}^{\mathrm{QCL}}$ is four. For SSB 1, up to three different candidate locations are possible and therefore must be measured.

SCS = 15 kHz	Half frame									
Subframe	1		2		3		4		5	
Slot	0		1		2		3		4	
SSB position	0	1	2	3	4	5	6	7	8	9
QCL = 4		SSB 1				SSB 1				SSB 1

Figure 18. The candidate locations for the SSB 1. SCS = 15 kHz and $N_{\mathrm{SSB}}^{\mathrm{QCL}} = 4$.

Figure 19 shows the same as the figure above, but the subcarrier spacing is changed from 15 kHz to 30 kHz. When the SCS is 30 kHz and the value of $N_{\mathrm{SSB}}^{\mathrm{QCL}}$ is four, up to five candidate locations must be measured.

SCS = 30 kHz	Half frame																			
Subframe	1				2				3				4				5			
Slot	1		2		3		4		5		6		7		8		9		10	
SSB position	0	1	2	3	4	5	6	7	8	9	10	11	12	13	14	15	16	17	18	19
QCL = 4		SSB 1				SSB 1				SSB 1				SSB 1				SSB 1		

Figure 19. Candidate locations for SSB 1. SCS = 30 kHz and $N_{\mathrm{SSB}}^{\mathrm{QCL}} = 4$.

Figure 20 shows candidate locations when the SCS is again 30 kHz but the value of $N_{\mathrm{SSB}}^{\mathrm{QCL}}$ is changed from four to one. The UE must measure up to 20 candidate locations to find the location for SSB 0.

SCS = 30 kHz	Half frame																			
Subframe	1				2				3				4				5			
Slot	1		2		3		4		5		6		7		8		9		10	
SSB position	0	1	2	3	4	5	6	7	8	9	10	11	12	13	14	15	16	17	18	19
QCL = 1	SSB 0	SSB 0	SSB 0	SSB 0	SSB 0	SSB 0	SSB 0	SSB 0	SSB 0	SSB 0	SSB 0	SSB 0	SSB 0	SSB 0	SSB 0	SSB 0	SSB 0	SSB 0	SSB 0	SSB 0

Figure 20. Candidate locations for SSB 1. SCS = 30 kHz and $N_{\mathrm{SSB}}^{\mathrm{QCL}} = 1$.

The examples above are simple and the situation becomes much more complex when there are up to eight different cells and 14 different SSBs to be measured as mentioned in Section 3.4. All eight cells could have either same or different $N_{\mathrm{SSB}}^{\mathrm{QCL}}$ values. Figure 21 visualizes the more practical combination of cells and SSBs. The figure highlights SSBs which the UE can see and therefore is able to performs measurements. It is notable that the UE may not see all possible beams for various reasons. Also, for example limitations of the UE capability can cut off some beams as for example only the strongest beams may be measured. The figure shows 98 different candidate locations which all must be measured to find the correct location of each SSB. In the worst-case scenario, there can be 160 different measurements, if all eight cells have $N_{\mathrm{SSB}}^{\mathrm{QCL}}$ value as one.

SCS = 30 kHz	Half frame																			
Subframe	1				2				3				4				5			
Slot	1		2		3		4		5		6		7		8		9		10	
SSB position	0	1	2	3	4	5	6	7	8	9	10	11	12	13	14	15	16	17	18	19
PCI = 1 QCL = 1	SSB 0	SSB 0	SSB 0	SSB 0	SSB 0	SSB 0	SSB 0	SSB 0	SSB 0	SSB 0	SSB 0	SSB 0	SSB 0	SSB 0	SSB 0	SSB 0	SSB 0	SSB 0	SSB 0	SSB 0
PCI = 2 QCL = 2	SSB 0	SSB 1	SSB 0	SSB 1	SSB 0	SSB 1	SSB 0	SSB 1	SSB 0	SSB 1	SSB 0	SSB 1	SSB 0	SSB 1	SSB 0	SSB 1	SSB 0	SSB 1	SSB 0	SSB 1
PCI = 3 QCL = 8		SSB 1	SSB 2	SSB 3						SSB 1	SSB 2	SSB 3						SSB 1	SSB 2	SSB 3
PCI = 4 QCL = 4				SSB 3				SSB 3				SSB 3				SSB 3				SSB 3
PCI = 5 QCL = 1	SSB 0	SSB 0	SSB 0	SSB 0	SSB 0	SSB 0	SSB 0	SSB 0	SSB 0	SSB 0	SSB 0	SSB 0	SSB 0	SSB 0	SSB 0	SSB 0	SSB 0	SSB 0	SSB 0	SSB 0
PCI = 6 QCL = 8	SSB 0	SSB 1	SSB 2						SSB 0	SSB 1	SSB 2						SSB 0	SSB 1	SSB 2	
PCI = 7 QCL = 8				SSB 3	SSB 4							SSB 3	SSB 4							SSB 3
PCI = 8 QCL = 2		SSB 1		SSB 1		SSB 1		SSB 1		SSB 1		SSB 1		SSB 1		SSB 1		SSB 1		SSB 1

Figure 21. The example of the SSB locations for eight cell and for 14 different SSB.

From the FW perspective, all candidate locations have already been captured by the MU and the FW is only searching which SSBs must be measured from the certain location. To know which SSB can be transmitted at the certain time, the UE should count each time when there is the possibility for the certain SSB. To find which candidate location is ongoing, the UE uses

$$SSB_{\mathrm{idx}} + \left(SSB_{\mathrm{count}} \times N_{\mathrm{SSB}}^{\mathrm{QCL}}\right), \tag{39}$$

where SSB_{idx} is the index of the SSB, for example, for SSB 0, the SSB index is zero. SSB_{count} is the number of the times that the certain candidate location for the SSB has been occurred, starting from zero and $N_{\mathrm{SSB}}^{\mathrm{QCL}}$ is QCL the value of the beam. Then fitting (39) to (38), it results

$$\left(SSB_{\mathrm{idx}} + \left(SSB_{\mathrm{count}} \times N_{\mathrm{SSB}}^{\mathrm{QCL}}\right)\right) \mathrm{mod}\left(N_{\mathrm{SSB}}^{\mathrm{QCL}}\right). \tag{40}$$

By comparing the result of (40) to the SSB index, the UE knows if this location can be the candidate location for the SSB.

After the SSBs are set into the queue, RSRP and SINR are calculated. According to Section 3.3, the RSRP is calculated by taking linear average over SSS symbol's subcarrier powers as

$$RSRP = \frac{1}{127}\sum_{k=56}^{182} p_{\mathrm{k}}, \tag{41}$$

where p_{k} is the power of the kth subcarrier. Then the SINR can be calculated by using

$$SINR = \frac{RSRP}{\frac{1}{127}\sum_{k=56}^{182}\left(\sigma_{\mathrm{k,n}}^2 + \sigma_{\mathrm{k,i}}^2\right)}, \tag{42}$$

where $\sigma_{\mathrm{k,n}}^2$ is a noise power and $\sigma_{\mathrm{k,i}}^2$ is a interference power at the kth subcarrier. The SINR is then used to detect the correct location of the SSB on the time domain.

When the FW finds which candidate location is the strongest one, the location index for the beam is found by dividing (39) by the $N_{\mathrm{SSB}}^{\mathrm{QCL}}$ and set it into floor function as

$$\left\lfloor \frac{(SSB_{\mathrm{idx}} + (SSB_{\mathrm{count}} * N_{\mathrm{SSB}}^{\mathrm{QCL}}))}{N_{\mathrm{SSB}}^{\mathrm{QCL}}} \right\rfloor. \tag{43}$$

This results always the value of zero for the first SSB occurring per SSB index X, where $0 \leq X \leq 7$. Table 12 visualizes the results of (43) per $N_{\mathrm{SSB}}^{\mathrm{QCL}}$ and per candidate location for each SSB index when the SCS is 15 kHz.

Table 12. The results of (43) per $N_{\mathrm{SSB}}^{\mathrm{QCL}}$ and candidate location.

$N_{\mathrm{SSB}}^{\mathrm{QCL}}$	Location	0	1	2	3	4	5	6	7	8	9	10
1		0	1	2	3	4	5	6	7	8	9	10
2		0	0	1	1	2	2	3	3	4	4	5
4		0	0	0	0	1	1	1	1	2	2	2
8		0	0	0	0	0	0	0	0	1	1	1

5.3 Tests and Environment

Testing is performed in a non-commercial testing environment. For this thesis, four different testing configurations are created per the SCS. The purpose of the testing is to test the NR-U implementation performance against legacy NR implementation. All configurations use either 15 kHz or 30 kHz SCS. First two test case configurations consider one cell and one beam case where the value of $N_{\mathrm{SSB}}^{\mathrm{QCL}}$ is either eight or one and these test cases are intended to refer the lightest and the heaviest measurements with one beam. These test cases are compared against NR test case which uses same subcarrier spaces and is built to measure only one beam. The third test case is intended to be the worst-case in NR-U. The case is built by using eight different beams, one for each cell which uses the $\mathrm{N}_{\mathrm{SSB}}^{\mathrm{QCL}}$ value of one. As the value of the $\mathrm{N}_{\mathrm{SSB}}^{\mathrm{QCL}}$ is one for all cells, total of 160 different measurements are performed and therefore test configuration is seen as the worst-case scenario. The worst-case test case is then compared to two different NR test cases where the first test case is supporting eight beams and the second one is supporting 14 different beams, which is the worst-case of the NR. In the last NR-U test case, only one candidate location is measured which is then compared to one NR beam measurement to see the costs between NR and NR-U implementation per a measurement. Table 13 summaries all test case configurations, where N_{beams} refers to the number of the beams in the test case.

Table 13. Test case configurations.

RAT	SCS	$N_{\mathrm{SSB}}^{\mathrm{QCL}}$	N_{beams}	Total measurements
NR-U	15 kHz	8	1	2
NR-U	15 kHz	1	1	10
NR-U	15 kHz	1	8	80
NR-U	30 kHz	8	1	3
NR-U	30 kHz	1	1	20
NR-U	30 kHz	1	8	160
NR-U	Both	8	1	1
NR	Both	-	1	1
NR	Both	-	8	8
NR	Both	-	14	14

Table 14 shows cases which are used for comparison between the NR implementation and the NR-U implementation. $N_{\mathrm{SSB\,locations,X}}$ tells the number of SSB locations which are measured with the implementation X. The cases in Table 14 are used only for the CPU load measurement. Last column tells the ratio of the measurement numbers between implementations.

Table 14. Test case comparison combinations.

Case name	SCS	$N_{\mathrm{SSB\,locations,NR}}$	$N_{\mathrm{SSB\,locations,NR-U}}$	The ratio of the measurements
Case 1	15 kHz	1	2	2
Case 2	15 kHz	1	10	10
Case 3	15 kHz	8	80	10
Case 4	15 kHz	14	80	5.714
Case 5	15 kHz	1	80	80
Case 6	15 kHz	1	1	1
Case 7	30 kHz	1	3	3
Case 8	30 kHz	1	20	20
Case 9	30 kHz	8	160	20
Case 10	30 kHz	14	160	11.429
Case 11	30 kHz	1	160	160
Case 12	30 kHz	1	1	1

6 RESULTS

In this chapter, the results of the tests are introduced. First, there is a short section for hypothesis of the research results and after the hypothesis, the results for the memory usage and the CPU load are presented.

6.1 Hypothesis of Research Results

The maximum number of the SSB candidate locations have increased from eight to 10 and 20, depending on the SCS as Table 15 shows. Other requirements about the measurement capabilities of the UE have stayed same between NR and NR-U: In the intra-frequency measurements at FR1, the UE should be able to perform measurements of up to eight cells and up to 14 different SSBs. In the inter-frequency measurements at FR1, the UE should be able to perform measurements of up to four cells and seven different SSBs.

Table 15. SSB location indices for NR and NR-U at FR1 region.

RAT	Case	SCS	SSB location indices
NR	A	15	2,8,16,22,30,36,44,50
NR	B	30	4,8,16,20,32,36,44,48
NR	C	30	2,8,16,22,30,36,44,50
NR-U	A	15	2,8,16,22,30,36,44,50,58,64
NR-U	C	30	2,8,16,22,30,36,44,50,58,64,72, 78,86,92,100,106,114,120,128,134

The fundamental of the SSB transmission is changed from NR to NR-U as QCL assumption is expanded for all SSBs within the transmission window. The change gives to a base station more freedom for transmission as in NR, the SSB transmission is periodic and therefore the locations of SSBs are locked. Expanding the QCL assumption offers more freedom for a transmitter to make time shift for SSBs if the periodic transmission is not possible as a channel could be shared with other RAT such as Wi-Fi.

Due to the fact of the increased number of the candidate locations and the QCL expansion, it is fair to assume that the load of the CPU will increase. Table 16 shows the number of the candidate locations for one SSB with 15 kHz SCS and with different $N_{\mathrm{SSB}}^{\mathrm{QCL}}$ values.

Table 16. QCL affect for the candidate locations at NR-U with 15 kHz SCS.

SCS	$N_{\mathrm{SSB}}^{\mathrm{QCL}}$	Candidate locations per SSB.	The maximum number of the candidate locations.
15 kHz	1	10	80
15 kHz	2	5	70
15 kHz	4	2 or 3	42
15 kHz	8	1 or 2	28

The table also shows the maximum number of the candidate locations if the maximum number of the beams are used. With the $N_{\mathrm{SSB}}^{\mathrm{QCL}}$ value of one, only eight beams are used while in all other $N_{\mathrm{SSB}}^{\mathrm{QCL}}$ values, 14 beams are used. With 15 kHz SCS and the maximum number of the beams, the UE must measure 28 to 80 different candidate locations, depending on used $N_{\mathrm{SSB}}^{\mathrm{QCL}}$. A NR-U device will always perform more measurements than a NR device except in the lightest cases.

For example, when comparing the worst-case scenario of NR-U against the worst-case scenario of NR, there would be around 5.7 times as many locations to be measured in NR-U as NR does. When comparing 14 beam NR measurement to 14 beam NR-U measurement with the $N_{\mathrm{SSB}}^{\mathrm{QCL}}$ value of eight, NR-U have two times as many locations to be measured as NR does. Appendix 2 shows examples how SSBs could be located on the time domain to get the maximum measurement numbers as shown in Table 16.

With 30 kHz SCS, the number of the candidate locations in the worst-case scenario is 160 as Table 17 shows.

Table 17. QCL affect for the candidate locations of the SSB at NR-U with 30 kHz SCS.

SCS	$N_{\mathrm{SSB}}^{\mathrm{QCL}}$	Candidate locations per SSB.	Maximum number of the candidate locations.
30 kHz	1	20	160
30 kHz	2	10	140
30 kHz	4	5	70
30 kHz	8	2 or 3	42

The table also shows the maximum number of the candidate locations if the maximum number of the beams are used. By changing the SCS from 15 kHz to 30 kHz, it basically doubles the number of the candidate locations. If the worst-case scenario of NR-U is then compared to the worst-case scenario of NR with 14 beams, NR-U measures around 11.4 times as much as NR does. Even in the scenario where $N_{\mathrm{SSB}}^{\mathrm{QCL}}$ value is eight and 14 beams are measured, NR-U have three times as many measurements to be performed as NR does. Appendix 3 shows examples how the SSBs could be located on the time domain to get the maximum measurement numbers as shown in Table 17.

From Table 16 and Table 17 it can be seen that the load of the CPU is at least doubled. The CPU load does not double if the used SSBs occur only once in the 15 kHz SCS with the QCL value of eight. Those SSBs have indices from two to seven. If only the ratio of the measurement numbers is analysed from Table 14, there should be a huge performance difference between the NR and the NR-U implementations. The analysis of the CPU load should also be applicable for the analysis of the memory usage. It is natural, that when make measurements for more locations, also need of the memory will increase.

6.2 Memory Usage

Two kind of the memory measurements are considered in this thesis. Firstly, a program memory measurement is done to investigate how much the NR-U code increases the program memory size compared to the NR implementation. It is natural that a new RAT implementation increases the amount of the code. Secondly, a data memory measurement is performed to see the effect of the NR-U measurements compared to the NR measurements. The data memory measurement is not an exact measurement but more like the consideration of required memory for the measurements. The data memory usage is more straightforward process as for every measurement, the certain amount of the memory for the data needs to be allocated. In this thesis, a block is used to descript the amount of the memory used for one measurement per a candidate location. For example, if only one beam is measured at the NR, it would take just one block of the memory. For the NR-U, there would be one to 20 memory blocks allocated for one beam, depending on the used configuration.

If simple static memory allocation per measurement is assumed, memory growth between the NR and the NR-U is linear. Figure 22 shows how the memory usage differs between the NR and the NR-U from the lightest to the heaviest usage with the different configurations. It can be clearly seen that in the one beam worst-case scenario, with 30 kHz SCS and with the $N_{\mathrm{SSB}}^{\mathrm{QCL}}$ value of one, the NR-U needs 20 times as much memory as the NR does to handle all the measurements of the beam. With 15 kHz SCS and the $N_{\mathrm{SSB}}^{\mathrm{QCL}}$ value of one, the NR-U needs ten times as much memory as the NR does. With the lightest-cases of the NR-U, the memory usage is at least doubled or tripled, depending on the used configuration.

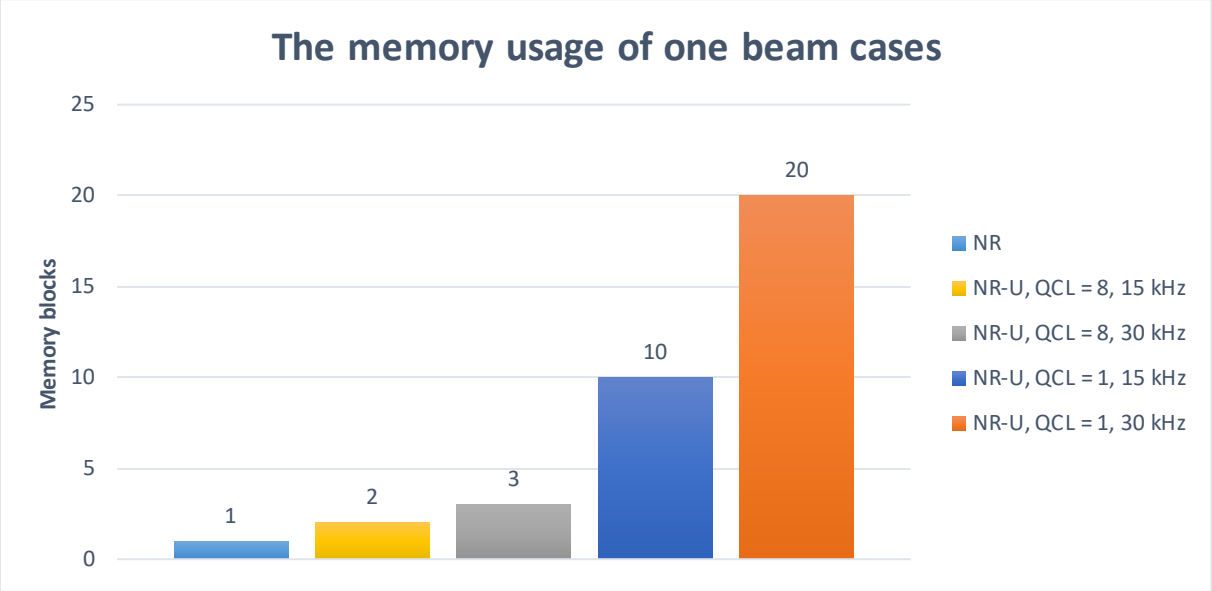

Figure 22. The memory usage in the NR versus the NR-U with one beam and different configurations.

Figure 23 shows the memory usage in the multi-beam worst-case scenarios with the different configurations. The NR-U scenarios in the figure are compared to the two different NR cases which use eight and 14 beams. The both NR-U cases use eight beams as the value of the $N_{\mathrm{SSB}}^{\mathrm{QCL}}$ is limiting the maximum number of the beams to one per a cell. The NR-U uses around 11.4 times as much memory with 30 kHz SCS when comparing to the NR case with 14 beams. If limiting the beam number to be equal in both RATs, the NR-U uses 20 times as much memory as the NR does. If comparing the memory usage with 15 kHz SCS, the NR-U uses 5.7 times as much memory as the NR does with 14 beams and if the number of the beams is decreased to eight in the NR so that the number of the NR beams equals with the number of the NR-U beams, the NR-U uses ten times as much memory as the NR does.

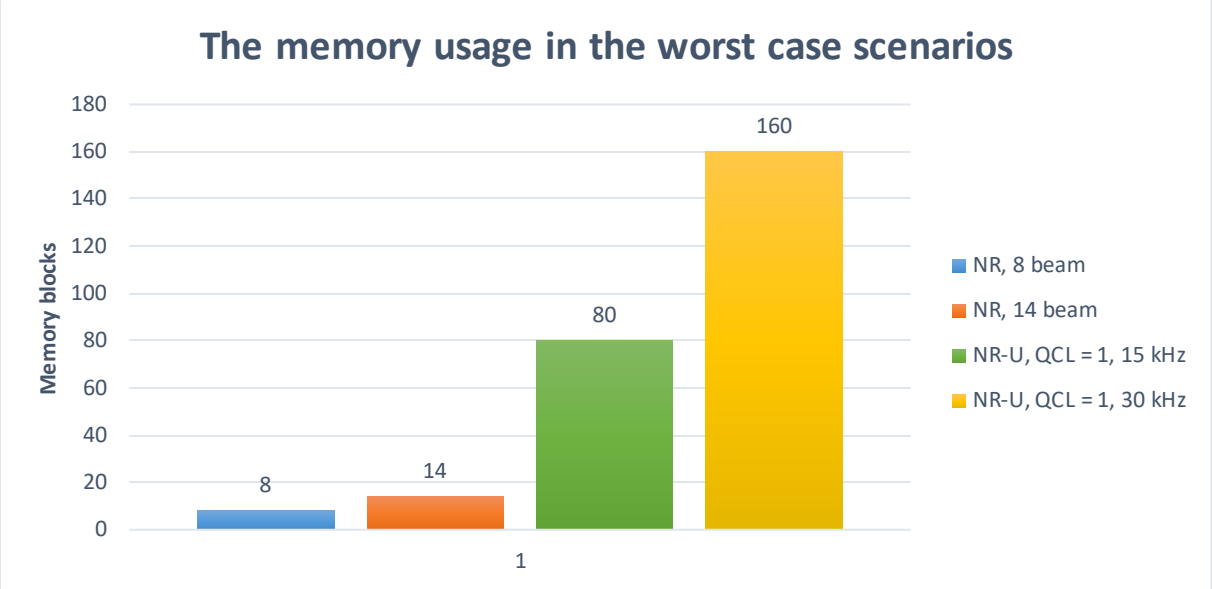

Figure 23. The memory usage in the worst-case scenarios between the NR and the NR-U with different configurations.

As a summary, Figure 22 and Figure 23 shows that if the static memory allocation is done, the NR-U may uses a lot more memory compared to the NR, especially when the value of the N_{SSB}^{QCL} is small. When the value of the N_{SSB}^{QCL} is increased, the UE uses a lot of less memory per beam for the measurements. For example, if the value of the N_{SSB}^{QCL} is eight, and 15 kHz SCS is used, there could be only one measurement more in the NR-U than in the NR and therefore the UE uses almost equal amount of the memory.

The program memory usage is measured by using a non-commercial tool which measures the size of the compiled code. The base level is the size of the NR implementation and it is then compared to the NR-U implementation. Figure 24 shows the results of the program memory sizes and it seems that new NR-U implementation increases the program memory size by around 5%. The program memory measurement does not consider other modules and how effectively the NR-U is implemented overall to the product.

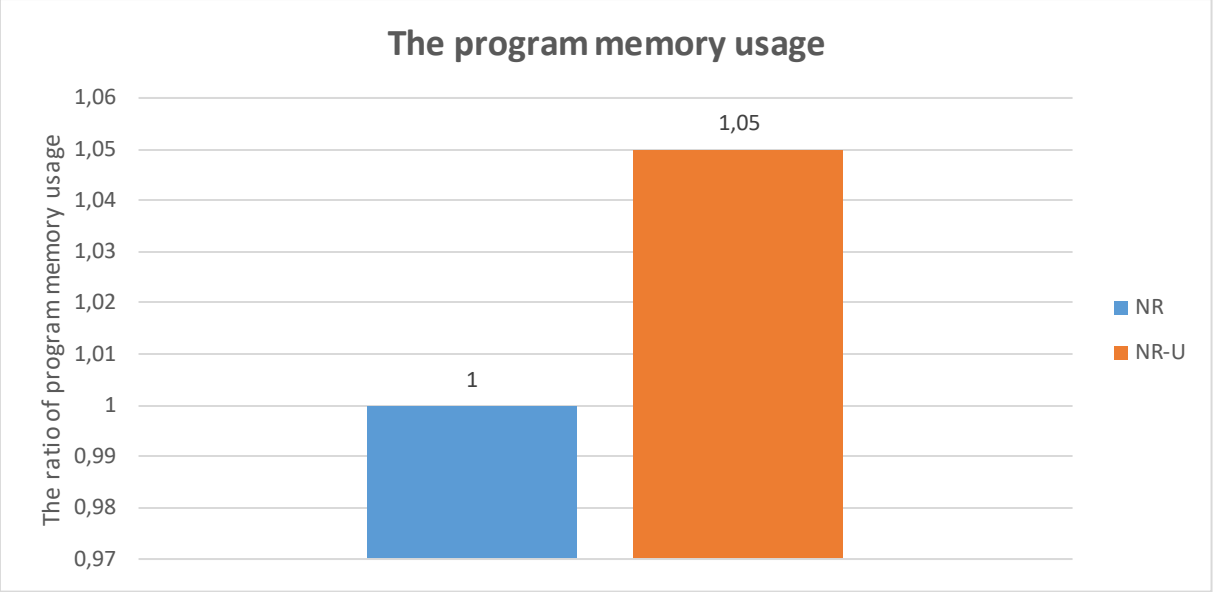

Figure 24. The program memory usage between the NR and the NR-U.

6.3 Central processing unit Usage

The CPU load is measured in cycles. Four test cases are created to simulate the NR-U cycle usage for both 15 kHz and 30 kHz SCS. First two test cases are used to compare one beam measurements between the NR-U and the NR where the NR-U uses different $N_{\mathrm{SSB}}^{\mathrm{QCL}}$ values. The third test case is used to compare the worst-case scenario of the NR-U to the NR where the cases are built by using eight and 14 beams. This is meant to be the worst-case of NR-U scenario against the scenario of NR where first are the equal number of beams and then the maximum number of beams. The results are given as the ratio between the NR and the NR-U, where the NR cycle usage is the base level. The last test case is used to compare the NR-U and the NR with one location measurement.

6.3.1 Cycle Usage with 15 kHz Subcarrier Spacing

Figure 25 shows the results of case 1 and case 2 from Table 14. With the $N_{\mathrm{SSB}}^{\mathrm{QCL}}$ value of eight, in the NR-U two times as many candidate locations are measured than in the NR but the NR-U uses 1.7 times as much cycles as the NR does. When the SSB is transmitted with the $N_{\mathrm{SSB}}^{\mathrm{QCL}}$ value of one, in the NR-U, ten times as many candidate locations are measured compared to the NR. Therefore, the cycle usage increases, and the NR-U uses six times as many cycles as the NR does for the measurements.

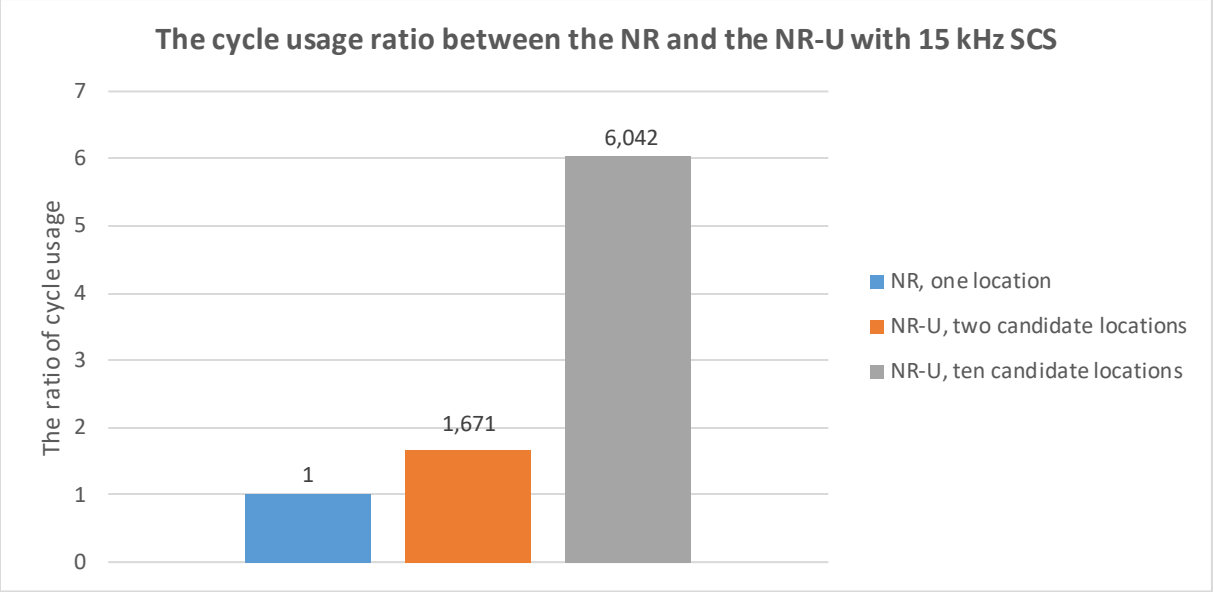

Figure 25. One beam cycle usage comparison between the NR and the NR-U with different NR-U configurations.

Figure 26 shows the result of case 3 from Table 14. The result of case 3 is giving the ratio of the cycle usage from the measurements of eight NR beams against eight NR-U cells which uses the $N_{\mathrm{SSB}}^{\mathrm{QCL}}$ value of one. The NR-U performs measurements for 80 candidate locations to find the locations for the SSBs. It seems that the NR-U uses 9.1 times as much cycles as the NR does for the measurements while the NR-U measures ten times as many candidate locations as the NR does.

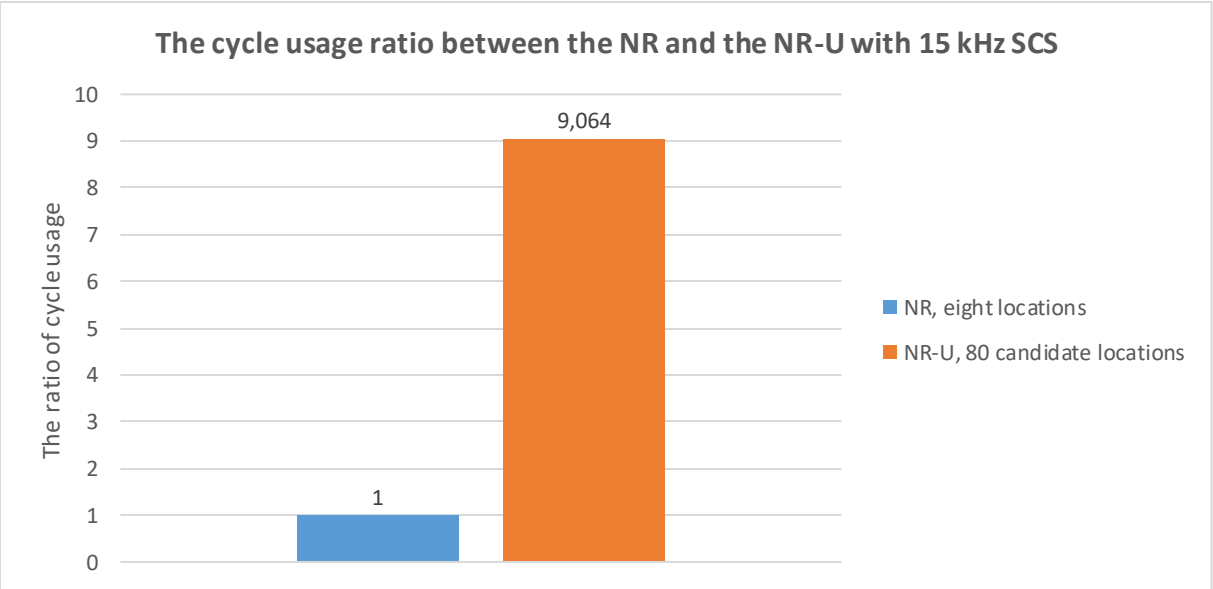

Figure 26. The cycle usage comparison between the NR, with eight beams, and the NR-U with eight cell and the $N_{\mathrm{SSB}}^{\mathrm{QCL}}$ value of one.

Figure 27 compares the worst-case scenario of the NR against the worst-case scenario of the NR-U. The result from the figure refers to case 4 from Table 14. This time the NR performs measurements for 14 different beams and the NR-U measures 8 cells with the $N_{\mathrm{SSB}}^{\mathrm{QCL}}$ value of

one. Therefore, the NR-U measures 5.7 times as many candidate locations as the NR does and the ratio of the cycle usage is almost equal to the ratio of the measurement times. The NR-U uses 5.4 times as much cycles as the NR does.

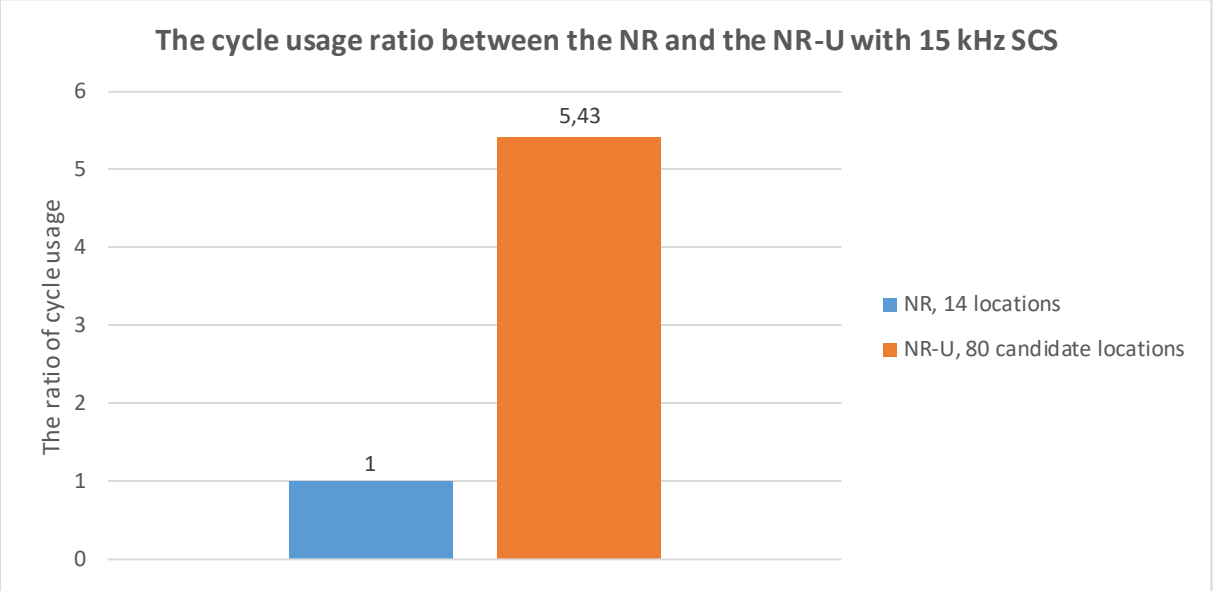

Figure 27. The cycle usage comparison between the NR, with 14 beams, and the NR-U with eight cell and the $N_{\mathrm{SSB}}^{\mathrm{QCL}}$ value of one.

Figure 28 shows the result of case 5 from Table 14. Now the NR measures only one beam and the NR-U measures 8 cells which gives 80 candidate locations as the value of the $N_{\mathrm{SSB}}^{\mathrm{QCL}}$ is one. While the NR-U performs measurements 80 times as many as the NR does, it seems that it uses only 44.6 times as much cycles as the NR does.

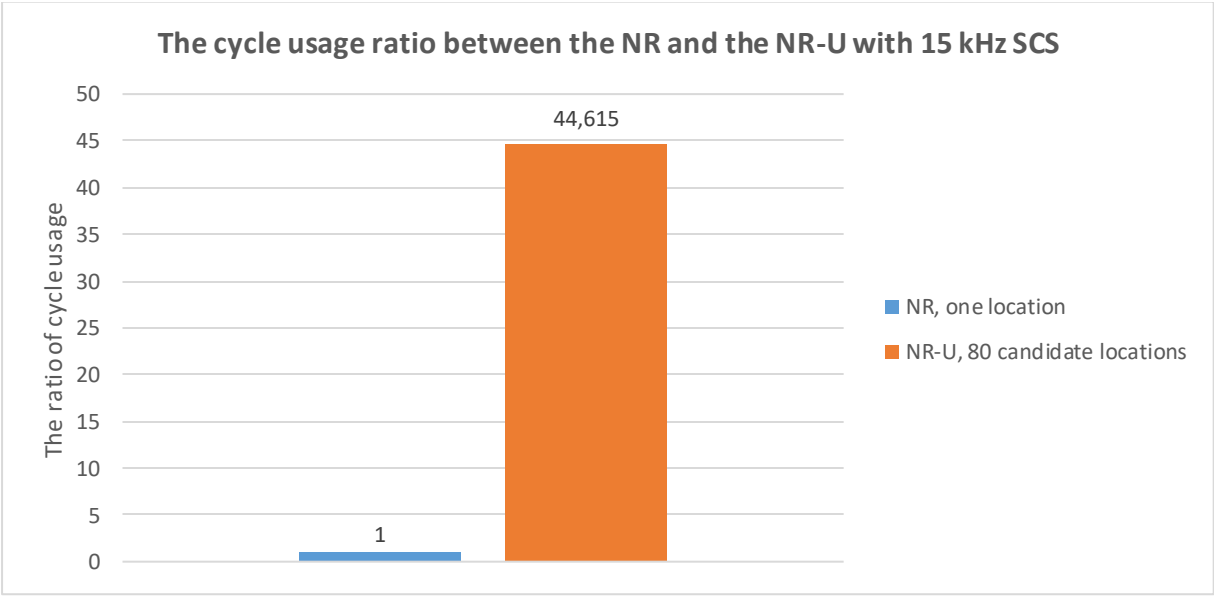

Figure 28. The cycle usage comparison between the NR, with one beam, and the NR-U with eight cell and the $N_{\mathrm{SSB}}^{\mathrm{QCL}}$ value of one.

6.3.2 Cycle Usage with 30 kHz Subcarrier Spacing

Figure 29 shows the results of case 7 and case 8 from Table 14. With the $N_{\mathrm{SSB}}^{\mathrm{QCL}}$ value of eight, the NR-U uses around 2.2 times as much cycles as the NR does, while the NR-U measures three times as many candidate locations as the NR does. When the NR-U change the $N_{\mathrm{SSB}}^{\mathrm{QCL}}$ value from eight to one, it uses around 11.5 times as much cycles as the NR does, but the NR-U measures 20 times as many candidate locations as the NR does.

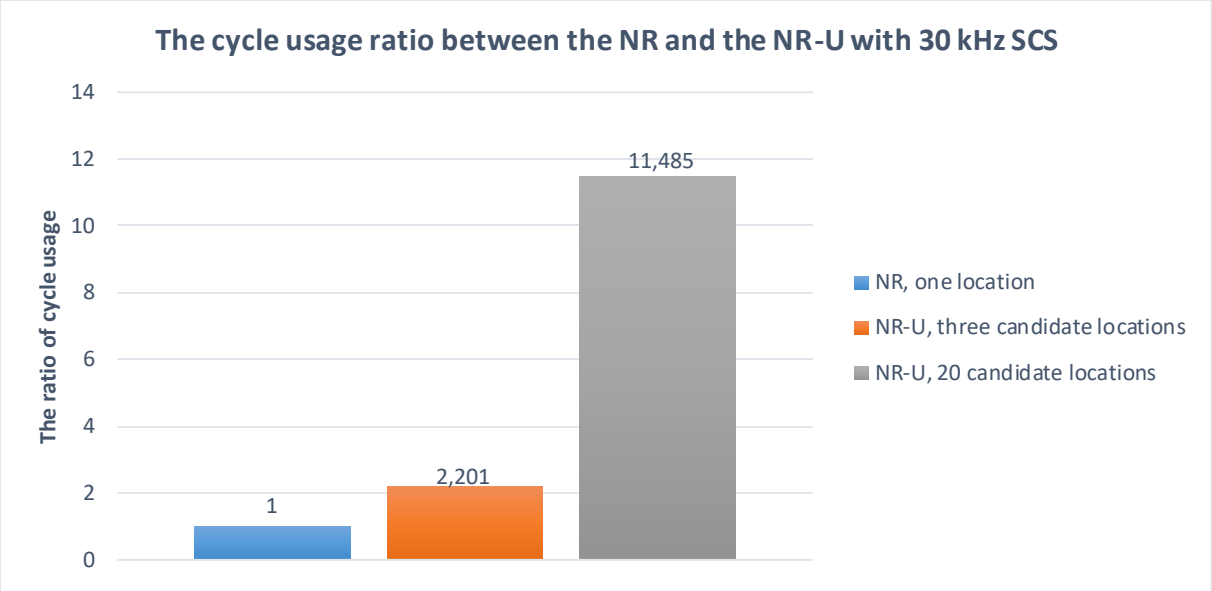

Figure 29. One beam cycle usage comparison between the NR and the NR-U with different NR-U configurations.

Figure 30 shows the ratio of the cycle usage when the NR perform measurements for eight beams while the NR-U performs measurements for eight cells with the $N_{\mathrm{SSB}}^{\mathrm{QCL}}$ value of one, which leads to 160 different measurements. The figure refers to the result of case 9 from Table 14 and it seems that the NR-U uses around 17.9 times as much cycles as the NR does, while the NR-U measures 20 times as many candidate locations as the NR does.

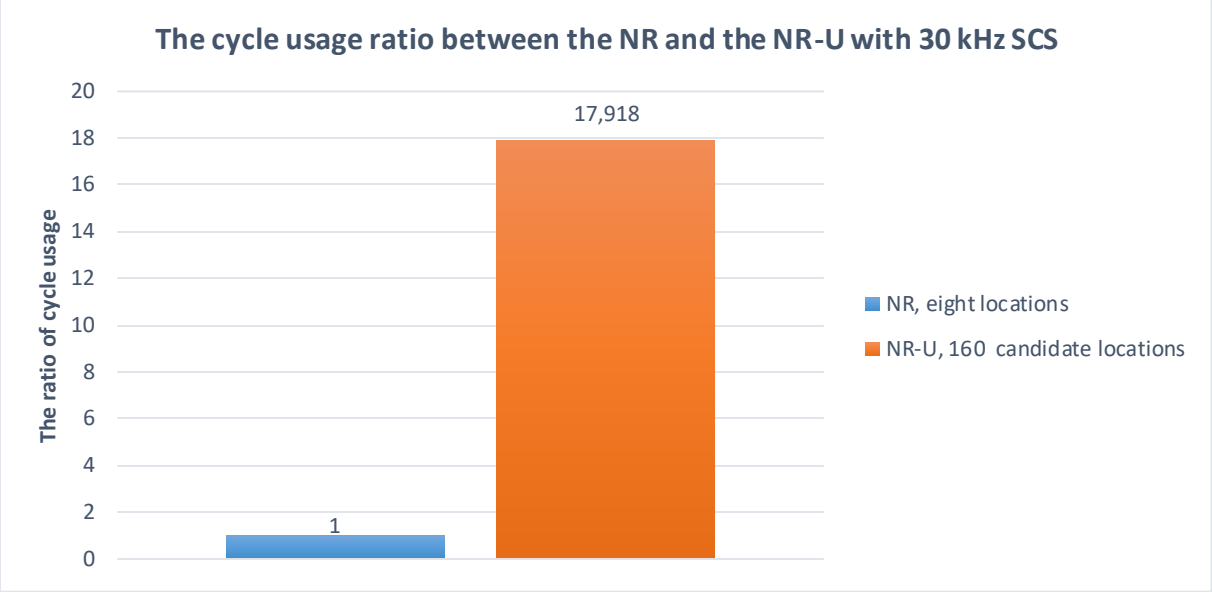

Figure 30. The cycle usage comparison between the NR, with eight beams, and the NR-U with eight cells and the $N_{\mathrm{SSB}}^{\mathrm{QCL}}$ value of one.

Figure 31 shows, when comparing the same NR-U configuration to the NR, which measures 14 beams, it seems that the NR-U uses 10.7 times as many cycles for the measurements as the NR does, while the NR-U measures 11.4 times as many candidate locations as the NR does. Figure 31 refers the result of case 10 from Table 14.

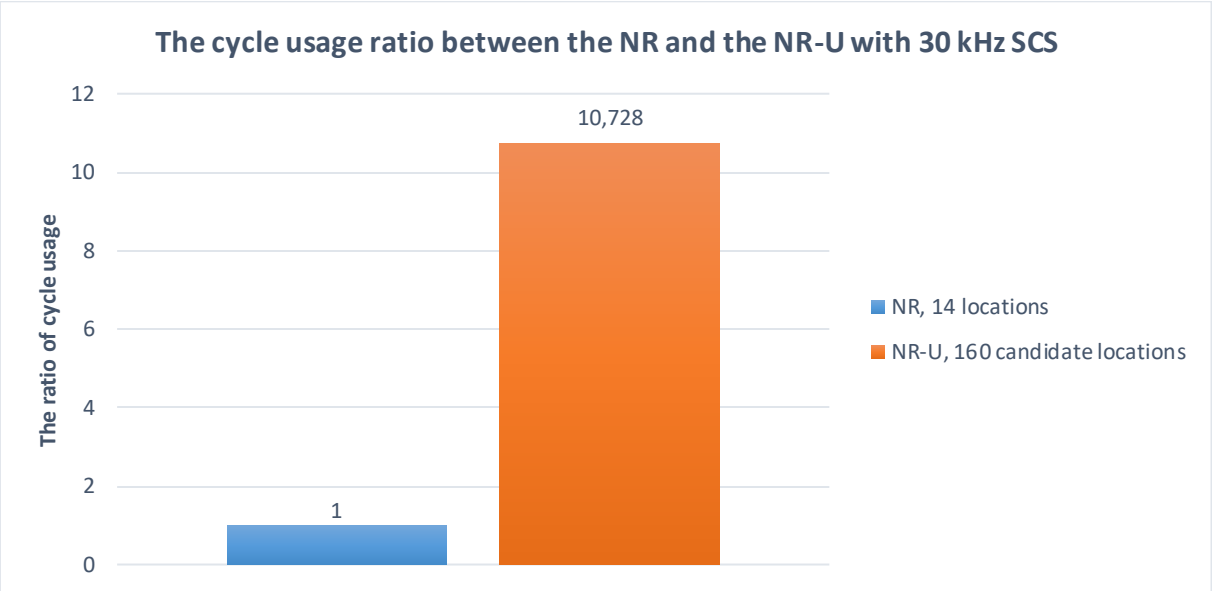

Figure 31. The cycle usage comparison between the NR, with 14 beams, and the NR-U with eight cells and the $N_{\mathrm{SSB}}^{\mathrm{QCL}}$ value of one.

Figure 32 shows the ratio of the cycle usage between the NR and the NR-U when the NR measures only one beam and the NR-U measures 160 different candidate locations. The figure shows the result of case 11 from Table 14. It seems that while the NR-U measures 160 times as many candidate locations as the NR does, the NR-U uses 88.1 times as much cycles as the NR does for the measurements.

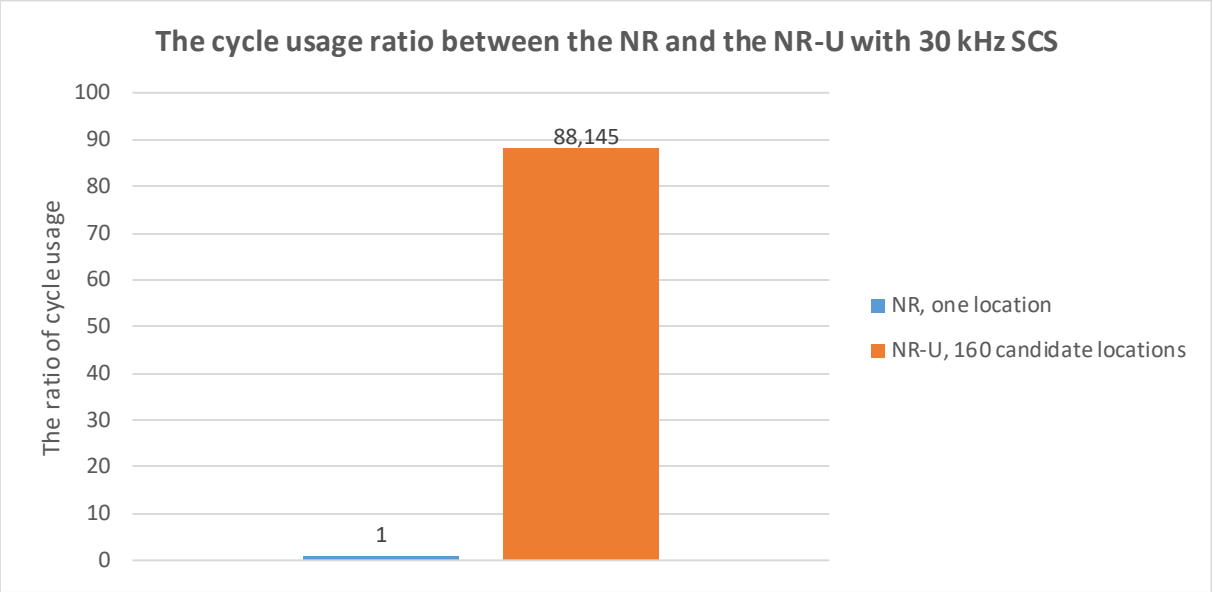

Figure 32. The cycle usage comparison between the NR, with one beam, and the NR-U with eight cells and the $N_{\mathrm{SSB}}^{\mathrm{QCL}}$ value of one.

6.3.3 Cycle Usage with One Candidate Location Measurement

The figures in Sections 6.3.1 and 6.3.2 shows that the cycle usage increases when the NR-U is used. Cases 6 and 12 compares one candidate location measurement in the NR-U to one beam measurement in the NR. Figure 33 shows that if the higher layer configures the FW to perform only one candidate location measurement, the NR-U uses 1.1 times as much cycles as the NR does for the measurement.

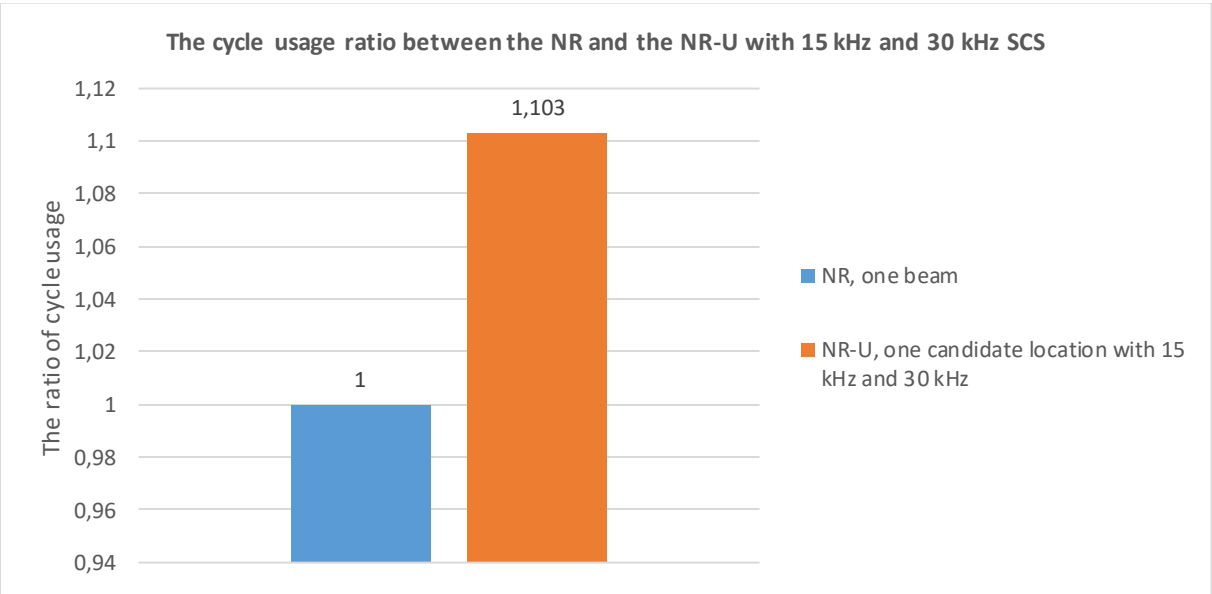

Figure 33. The cycle usage comparison between the NR, with one beam, and the NR-U with only one candidate location measurement.

10% increase is not desirable. This becomes from the fact that the NR-U specific solutions are including some complex tasks and those solutions increases the load of the CPU.

However, the cycle usage does not increase linearly with the number of the candidate locations. From the conclusion above it could be assumed that every candidate location measurement in the NR-U uses 10% more cycles compared to the NR. For example, if the NR-U measures ten times as many candidate locations as the NR, it could lead to 11 times as much cycle usage as the NR does. However, for example, in case 1 and case 7, there are two candidate locations when using 15 kHz SCS and three candidate locations when using 30 kHz SCS, but still the cycle usage stays below the ratio of the measurement times. The same effect is seen with case 5 and 11 where the NR performs measurements for only one beam and the NR-U measures 80 and 160 candidate locations. If the cycle usage would increase by 10% for every candidate location, this could mean that the NR-U would use 88 or 176 times as much cycles as the NR does. However, it does not. The ratio of the cycle usage is about half from the ratio of the measurement times and the ratio of the cycle usage does not increase above the ratio of the measurement times in any other case than in case 6 and in case 12. Table 18 shows the ratio of the cycle usage and the ratio of the measurement times.

Table 18. The ratio of the cycle usage and the ratio of the number of the measurements

Case Name	The ratio of the cycle usage	The ratio of the measurement times
Case 1	1.671	2
Case 2	6.042	10
Case 3	9.064	10
Case 4	5.43	5.714
Case 5	44.615	80
Case 6	1.103	1
Case 7	2.201	3
Case 8	11.485	20
Case 9	17.907	20
Case 10	10.728	11.429
Case 11	88.145	160
Case 12	1.103	1

In some multi-beam cases the ratio of the cycle usage increases to be close to the ratio of the measurement times, but it does not cross that. It seems that the larger ratio of the measurement times, the smaller ratio of the cycle usage is in relation to the single location measurement. The cycle usage decrease is due to the amount of common code in the implementation as the common code does not multiply with the number of candidate locations. Figure 34 illustrates the averaged cycle usage per one SSB location with different configurations.

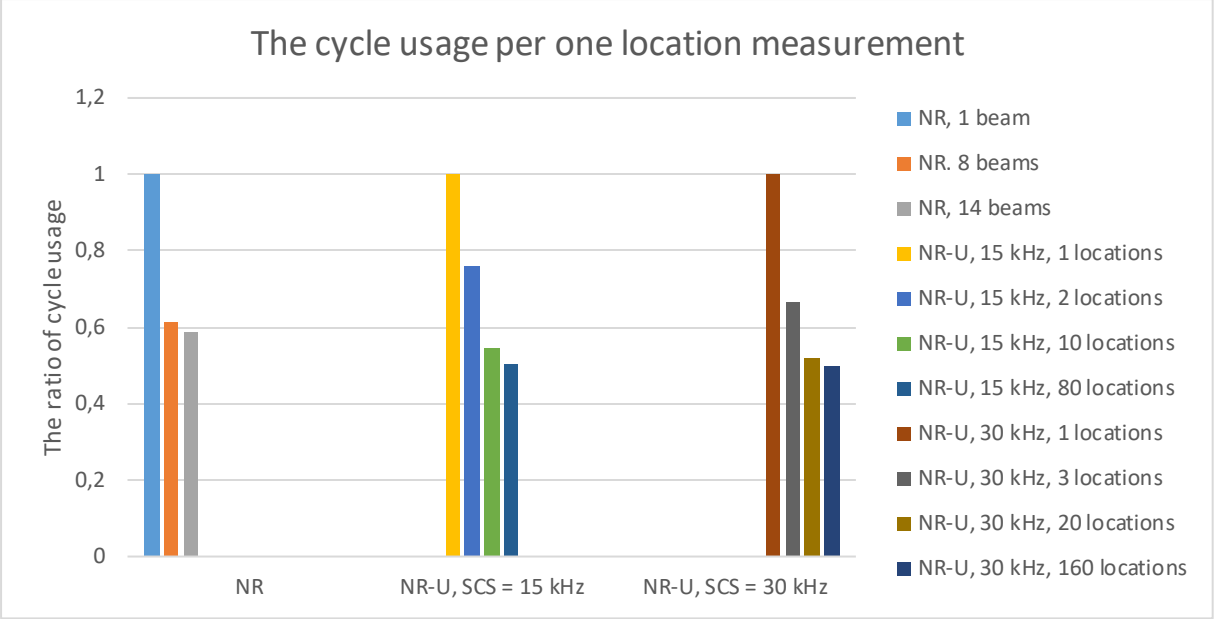

Figure 34. The ratio of the averaged cycle usage with different configurations per one location.

In each group, one beam or one candidate location measurement is seen as the base for the other configurations. In the first group, only the NR measurement have been shown. The averaged cycle usage per one measurement will drop when more beams are measured. The same effect is also seen with the second and the third groups which shows the averaged cycle usage per one candidate location of the NR-U measurements.

7 DISCUSSION

The focus for the thesis was to study how NR-U differs from NR and how the NR-U affects to memory usage and to cycle usage. The memory usage and the cycle usage were chosen as the key indicators to measure the performance of the NR-U implementation and as the NR-U is a new RAT it is natural to compare the results to the legacy NR implementation. As an answer to the use of the memories, there were two kind of the memory usages reviewed. The first measurement was how much a data memory may be used for cell measurements with the different NR-U configurations. The results showed that the data memory use increase linearly with the number of the candidate locations. When assuming that data memory allocation is done statically, there was no need to perform actual measurements, but calculation was done by hand. Different configurations need the different amount of the memory and therefore the memory analyses were focused only to the used data memory size. The second memory measurement was to show how the implementation increases the program memory size. This was presented by using a non-commercial tool and it was shown that the NR-U implementation increases the program memory size by around 5%. When considering the NR-U as the new RAT, it can be concluded that the implementation can reuse a lot of the NR code. Therefore, it is fair to say that the NR-U has minimal impact to the program memory usage and the NR-U needs only some specific solutions. The second key indicator was a CPU load which is measured in cycles by using a non-commercial tool. In one candidate location measurement, the cycle usage increased by 10%. However, 10% increase of the cycle usage did not repeat with every candidate location measurement. The results indicates that the NR-U implementation have a lot of common code, so the cycle consumption does not multiply by the number of candidate locations and therefore the cycle usage per one measurement is decreased as the function of the number of the candidate locations. For example, one location measurement cost less in the NR-U when the value of the $\square_{\mathrm{SSB}}^{\mathrm{QCL}}$ is less than eight.

Section 6.1 introduced the hypothesis of the research. It was shown that in theory, the memory usage and the CPU load should increase a lot and there could be a huge difference between the NR and the NR-U. The results show that in the memory usage, the theory may correspond well with the achieved results but with the cycle usage, the implementation performs better than expected. When also considering the change of the program memory size to the overall estimation of success, it could be said that the implementation has been successful. The cycle usage does not increase uncontrollably. However, the thesis still left doors open for some improvements and optimizations.

For simplicity, the simulation cases of the thesis were built by assuming that the UE is receiving the SSBs one by one which increases the load of the device a lot. In practice, it is more probable that the measurements of the SSBs could be done in groups. This requires that two or multiple SSBs are located close of each other so that the UE could perform measurements from the same captured data. To achieve accurate measurements from one data capturing, a device could use, for example, successive interference cancellation (SIC) to demodulate and decode all data one by one from one data capturing [11]. For example, in Figure 35, the SSBs are located close enough so that UE could capture both symbols at the same time. However, the SS symbols do interference each other but it can be reduced with, for example, SIC and by assuming that the SS symbol have low correlation between other SS symbols.

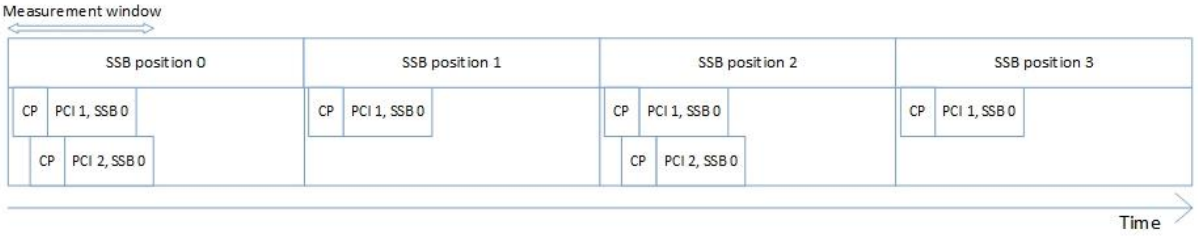

Figure 35. Simplified version of the measurement windows for PCI 1 and PCI 2 SSB 0.

The idea of grouping is studied more deeply. In order to do the grouping, the maximum difference between two symbols must be the length of CP. Figure 36 visualizes the idea of the grouping. If MU captures data for long enough, it is possible for the MU to capture the data of two beams at once and then separate SSBs from the data by using SIC where the strongest beam is measured first and then it is cancelled from the data so that the weaker one can be measured more accurately. Also, as SSS symbol have low auto and cross-correlation between other SSS symbols, wrong cell ID estimation is less probable.

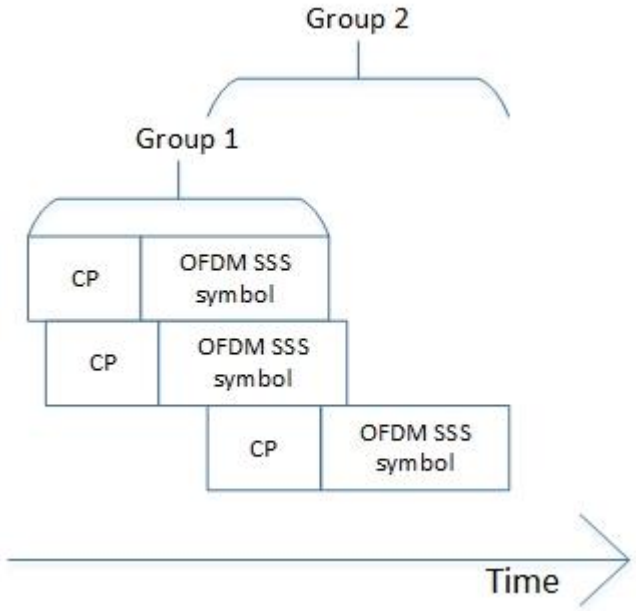

Figure 36. Visualization of grouping idea.

If multiple symbols are within the CP duration, a device could capture multiple beams at once to the same memory block. For example, if there are eight cells (eight beams) to be measured with the $N_{\mathrm{SSB}}^{\mathrm{QCL}}$ value of one and 15 kHz SCS is used, there could be 80 individual candidate locations. But using the theory above, the device could capture, for example, 20 data samples, two data samples from each ten candidate locations. If the SSBs are located close enough of each other, it could be possible to capture the data of all the locations, for example, within 20 groups instead of 80 individual data captures. Therefore, in this example, there would be two groups per location and all the SSBs could be measured from one of those two groups. However, there are still 80 measurements to be performed, but it would save a lot of the data memory when there is data only, for example, from 20 locations saved. So instead, that device uses 80 memory blocks for the measurements, it could only need, for example, 20 memory

blocks to find the locations for all eight SSBs. However, the worst-case scenario is still there where the UE needs to save all 80 captured data samples for the measurements.

The cycle usage of the CPU in this thesis represents absolute cycle values where the cell measurement module in the CPU is executing instructions. The results do not consider cycles which come, for example, from memory latencies. There are different kind of memories which have different latencies. Some of memories have shorter latencies which consumes less cycles and some, in other hand, have longer latencies which takes more cycles. The impacts of the different memories are not considered in this thesis as they are hard to simulate correctly, and many things affect to how the UE behaves. For example, other modules with higher priorities could need those faster memories, which means that the data of lower priority tasks need to be moved to the slower memory which then may increase the total cycle usage significantly. Because of that, the cycles which are hardware or priority related, are not considered here, but it is good to notice that in practice, depending on, for example, the FW module priority and memory architecture, the FW part of the cell measurement could consume a lot more time and therefore increase the load of the device much more than the results present. With a good overall design of the FW from the perspective of the priorities and memory implementation, it is possible to improve the cycle usage in all sectors.

In 3GPP meeting in 2019, it was decided to expand the NR spectrum to up to 71 GHz and the NR-U spectrum to up to 60 GHz which is named FR2-2 region. It was also decided to create one or more numerologies and support for up to 64 beams for both licensed and unlicensed bands. Some of the early versions of Release 17 specifications were published before the thesis was completed. TS 38.211 Release 17 introduced two new subcarrier spacing for the FR2-2 region: 480 kHz and 960 kHz. Also, a new number of the candidate locations are introduced, and the number of the candidate locations have been increased to 64, which is the same as the number of beams. The NR-U in the FR2-2 region differs a bit from the NR-U in the FR1 region as in the FR2-2, every candidate location can be filled with individual SSB. This leads to the change of the possible values of the $N_{\mathrm{SSB}}^{\mathrm{QCL}}$. For now, in the FR2-2 region, $N_{\mathrm{SSB}}^{\mathrm{QCL}}$ could be either 16, 32 or 64. [27] [28] [29] [30]

Capability of the UE in FR2-2 frequency region is not yet presented. However, if take, for example, intra-frequency FR2 measurement capability requirements from the version of Release 16, the UE should be able to measure up to six cells and 24 different SSBs [7]. For example, with the $N_{\mathrm{SSB}}^{\mathrm{QCL}}$ value of 16 and two cells, 24 different SSBs could be transmitted. This means, that the UE must perform measurements for 96 candidate locations to find the locations for 24 different SSBs. For now, it seems that in the future the NR-U in the FR2-2 region could be lighter version than the NR-U in the FR1 region in the view of the thesis. However, as the UE will operate in millimetre wave (mmWave) region, overall demands and loads of the UE could differs a lot from the UE which operate in the FR1 region.

Next research topic could be CSI-RS feasibility in the NR-U cell measurement and then compare the performance of the CSI-RS cell measurement to the performance of the SSB cell measurement. In this thesis, it is shown that the cell measurement from the SSB increases the memory usage and the load of the CPU so it could be interesting to see how much the load and memory usage of cell measurement of the CSI-RS differs to cell measurement of the SSB. It would also be interesting to see how LBT, different COTs and channel access procedures really affect to the SSB transmission. Also, field performance comparison between the NR and the NR-U products could be interesting topic. How much heavier the cell measurement is in the NR-U than in the NR in real application and in real environment.

8 SUMMARY

The purpose of this thesis was to develop firmware which performs cell measurement in 5G unlicenced spectrum. The implementation was tested in the non-commercial test environment and the memory and the cycle usage were decided to be so called key indicators for the performance analysis. To achieve the goal, the research started by studying the theory of the physical layer. The theory included the physical channels and the signals of downlink, the numerology, and the frame structure of the 5G NR as well as the resource grid. The theory of the physical layer also included the short theory of the OFDM symbols and the example of the SSB detection. After the theory of the physical layer, the thesis focused to the cell measurement procedure of the 5G NR in high level with the deeper review of the SSB, the parameters of the cell measurement and the requirements. Also, differences in the cell measurements between the NR and the NR-U was studied. The main difference between the NR and the NR-U was the fair coexistence with other RATs which may affect to the periodicity of the SSB transmission. In the unlicensed spectrum, also the other technologies could use the wireless medium, not just 5G NR base stations and 5G NR compatible devices. Because the unlicensed channel can be used a RAT which is not 3GPP compatible, the LBT was introduced. This leads to new channel access techniques which are based on LBT. Also, expanded QCL assumption between the SSBs were introduced to offer more freedom to the SSB transmissions by enabling time shift of the SSB. Also, to allow more space on time domain, the number of the candidate locations was increased from eight to 10 and 20.

The implementation was tested with 15 kHz and 30 kHz SCS. For both SCS, six different cases were created. Each case was intended to compare the NR-U implementation performance to the legacy NR. The results show that the memory usage of the NR-U implementation increases linearly as the function of the candidate locations. However, the program memory increased only by 5%. The CPU usage was measured in the cycles and it was shown that the cycle usage increased when compared the NR-U to the NR. In one location measurement, the cycle usage increased by 10% but the increase was not linear when there were more locations to measure. For example, in the worst-case scenario with 30 kHz SCS, the cycle usage stays on acceptable level as the NR-U uses around 88 times as much cycles as the NR does while the NR-U measures 160 times as many candidate locations as the NR does. Therefore, the cycle usage in the implementation stays at controllable level, and when performed the measurements for more candidate locations, less cycles was used per candidate location. Observations from the program memory and the cycle usage led to conclusion that the NR-U reused a lot of the legacy NR code and the common code were not used as the function of the candidate locations. It was stated that the implementation is stable and performs well. However, the tests did not consider, for example, memory latencies, grouping of the SSBs on time domain or other modules in the device. Some of those are hard to simulate accurately and could have a huge impact to device's performance in the view of memory and cycle consumption.

In the future the NR-U will have more frequencies as in 3GPP meeting it has been decided that the NR-U would be capable to operate in the FR2-2 frequency region. However, the FR2-2 frequency region expansion is not only area what future research could study. In the NR, there is possibility to perform cell measurements also from the CSI-RS. This could be one of many interested topics in the future NR-U study as it would be interesting to see if the CSI-RS can be more efficient in the NR-U cell measurement than cell measurement from the SSB.

9 REFERENCES

[1] 3GPP (read 16.9.2021). Release 16. URL: https://www.3gpp.org/release-16.

[2] 3GPP (2021). Release 16 Description; Summary of Rel-16 Work Items. Technical Report 21.916, Version 16.0.1, Release 16.

[3] E. Dahlman, S. Parkvall and J. Sköld, 5G NR: The Next Generation Wireless Access Technology, London, San Diego, Cambridge, Oxford: Elsevier Ltd, 2021.

[4] G. Naik, J.-M. Park, J. Ashdown and W. Lehr, "Next Generation Wi-Fi and 5G NR-U in the 6 GHz Bands: Opportunities and Challenges," in *IEEE Access,* vol. 8, pp. 153027 - 153056, 31 August 2020.

[5] S. Lagen, L. Giupponi, S. Goyal, N. Patriciello, B. Bojovic, A. Demir and M. Beluri, "New Radio Beam-Based Access to Unlicensed Spectrum: Design Challenges and Solutions," in *IEEE Communications Surveys & Tutorials,* vol. 22, no. 1, pp. 8-37, 2019.

[6] 3GPP (2018). Study on NR-based access to unlicensed spectrum. Technical Report 38.889, Version 16.0.0, Release 16.

[7] 3GPP (2021). Requirements for support of radio resource management. Technical Specification 38.133, Version 17.2.0, Release 17.

[8] 3GPP (2021). Physical Layer procedures for shared spectrum channel access. Technical Specification 37.213, Version 16.6.0, Release 16.

[9] X. Zhang (read 12.11.2021). How does support for unlicensed spectrum with NR-U transform what 5G can do for you? URL: https://www.qualcomm.com/news/onq/2020/06/11/how-does-support-unlicensed-spectrum-nr-u-transform-what-5g-can-do-you.

[10] Y. Wei and X. Zhang (read 12.11.2021). How does unlicensed spectrum with NR-U transform what 5G can do for you? URL: https://www.qualcomm.com/media/documents/files/presentation-how-nr-u-can-transform-what-5g-can-do-for-you.pdf.

[11] A. Zaidi, F. Athley, J. Medbo, U. Gustavsson, G. Durisi and X. Chen, 5G Physical Layer: Principles, Models and Technology Components, London, San Diego, Cambridge, Oxford: Elsevier Ltd, 2018.

[12] 3GPP (2021). Physical channels and modulation. Technical Specification 38.211, Version 16.6.0, Release 16.

[13] 3GPP (2021). NR and NG-RAN Overall description; Stage-2. Technical Specification 38.300, Version 16.6.0, Release 16.

[14] 3GPP (2021). User Equipment (UE) radio transmission and reception; Part 1: Range 1 Standalone. Technical Specification 38.101-1, Version 17.2.0, Release 17.

[15] 3GPP (2021). Radio Resource Control (RRC) protocol specification. Technical Specification 38.331, Version 16.6.0, Release 16.

[16] 3GPP (2022). System architecture for the 5G System (5GS). Technical Specification 23.501, Version 17.4.0, Release 17.

[17] A. Omri, M. Shaqfeh, A. Ali and H. Alnuweiri, "Synchronization Procedure in 5G NR Systems," in *IEEE Access,* vol. 7, pp. 41286 - 41295, 28 03 2019.

[18] P. Wang and F. Berggren, "Secondary Synchronization Signal in 5G New Radio," in *2018 IEEE International Conference on Communications (ICC)*, Kansas City, MO, USA, 2018.

[19] GSMA (read 15.11.2021). 5G TDD synchronisation Guidelines and Recommendations for the Coexistence of TDD Networks in the 3.5 GHz Range. URL: https://www.gsma.com/spectrum/wp-content/uploads/2020/04/3.5-GHz-5G-TDD-Synchronisation.pdf.

[20] 3GPP (2021). Physical layer procedures for control. Technical Specification 38.213, Version 16.6.0, Release 16.

[21] 3GPP (2021). Physical channels and modulation. Technical Specifications 36.211, Version 17.0.0, Release 17.

[22] Y.-H. You, J.-H. Park and I.-Y. Ahn, "Complexity Effective Sequential Detection of Secondary Synchronization Signal for 5G New Radio Communication Systems," in *IEEE Systems Journal,* vol. 15, no. 3, pp. 3382 - 3390, 2020.

[23] 3GPP (2021). Physical Layer Measurements. Technical Specification 38.215, Version 16.4.0, Release 16.

[24] M. Hirzallah, M. Krunz, B. Kecicioglu and B. Hamzeh, "5G New Radio Unlicensed: Challenges and Evaluation," in *IEEE Transactions on Cognitive Communications and Networking,* vol. 7, no. 3, pp. 689-701, 2021.

[25] J. Oh, Y. Kim, Y. Li, J. Bang and J. Lee, "Expanding 5G New Radio Technology to Unlicensed Spectrum," in *2019 IEEE Globecom Workshops (GC Wkshps)*, Waikoloa, HI, USA, 2020.

[26] 3GPP (2021). Physical Layer Procedures for data. Technical Specification 38.214, Version 16.7.0, Release 16.

[27] RP-193229 (2019). New WID on Extending current NR operation to 71 GHz. 3GPP TSG RAN Meeting #86. Sitges, Spain.

[28] Qualcomm (read 25.3.2022). Just in: 3GPP completes 5G NR Release 17. URL: https://www.qualcomm.com/news/onq/2022/03/24/just-3gpp-completes-5g-nr-release-17.

[29] 3GPP (2022). Physical channels and modulation. Technical Specification 38.211, Version 17.0.0, Release 17.

[30] 3GPP (2022). Physical layer procedures for control. Technical Specification 38.213, Version 17.0.0, Release 17.

10 APPENDICES

Appendix 1 NR slot format.
Appendix 2 An example for SSB candidate locations with 15 kHz subcarrier spacing to get the maximum number of measurements. Number in coloured element refers the index of SSB.
Appendix 3 An example for SSB candidate locations with 30 kHz subcarrier spacing to get the maximum number of measurements. Number in coloured element refers the index of SSB.

Appendix 1 NR slot format.

Format	Symbol number in a slot													
	0	1	2	3	4	5	6	7	8	9	10	11	12	13
0	DL	DL	DL	DL	DL	DL	DL	DL	DL	DL	DL	DL	DL	DL
1	UL	UL	UL	UL	UL	UL	UL	UL	UL	UL	UL	UL	UL	UL
2	F	F	F	F	F	F	F	F	F	F	F	F	F	F
3	DL	DL	DL	DL	DL	DL	DL	DL	DL	DL	DL	DL	DL	F
4	DL	DL	DL	DL	DL	DL	DL	DL	DL	DL	DL	DL	F	F
5	DL	DL	DL	DL	DL	DL	DL	DL	DL	DL	DL	F	F	F
6	DL	DL	DL	DL	DL	DL	DL	DL	DL	DL	F	F	F	F
7	DL	DL	DL	DL	DL	DL	DL	DL	DL	F	F	F	F	F
8	F	F	F	F	F	F	F	F	F	F	F	F	F	UL
9	F	F	F	F	F	F	F	F	F	F	F	F	UL	UL
10	F	UL	UL	UL	UL	UL	UL	UL	UL	UL	UL	UL	UL	UL
11	F	F	UL	UL	UL	UL	UL	UL	UL	UL	UL	UL	UL	UL
12	F	F	F	UL	UL	UL	UL	UL	UL	UL	UL	UL	UL	UL
13	F	F	F	F	UL	UL	UL	UL	UL	UL	UL	UL	UL	UL
14	F	F	F	F	F	UL	UL	UL	UL	UL	UL	UL	UL	UL
15	F	F	F	F	F	F	UL	UL	UL	UL	UL	UL	UL	UL
16	DL	F	F	F	F	F	F	F	F	F	F	F	F	F
17	DL	DL	F	F	F	F	F	F	F	F	F	F	F	F
18	DL	DL	DL	F	F	F	F	F	F	F	F	F	F	F
19	DL	F	F	F	F	F	F	F	F	F	F	F	F	UL
20	DL	DL	F	F	F	F	F	F	F	F	F	F	F	UL
21	DL	DL	DL	F	F	F	F	F	F	F	F	F	F	UL
22	DL	F	F	F	F	F	F	F	F	F	F	F	UL	UL
23	DL	DL	F	F	F	F	F	F	F	F	F	F	UL	UL
24	DL	DL	DL	F	F	F	F	F	F	F	F	F	UL	UL
25	DL	F	F	F	F	F	F	F	F	F	F	UL	UL	UL
26	DL	DL	F	F	F	F	F	F	F	F	F	UL	UL	UL
27	DL	DL	DL	F	F	F	F	F	F	F	F	UL	UL	UL
28	DL	DL	DL	DL	DL	DL	DL	DL	DL	DL	DL	DL	F	UL
29	DL	DL	DL	DL	DL	DL	DL	DL	DL	DL	DL	F	F	UL
30	DL	DL	DL	DL	DL	DL	DL	DL	DL	DL	F	F	F	UL
31	DL	DL	DL	DL	DL	DL	DL	DL	DL	DL	DL	F	UL	UL
32	DL	DL	DL	DL	DL	DL	DL	DL	DL	DL	F	F	UL	UL
33	DL	DL	DL	DL	DL	DL	DL	DL	DL	F	F	F	UL	UL
34	DL	F	UL	UL	UL	UL	UL	UL	UL	UL	UL	UL	UL	UL
35	DL	DL	F	UL	UL	UL	UL	UL	UL	UL	UL	UL	UL	UL
36	DL	DL	DL	F	UL	UL	UL	UL	UL	UL	UL	UL	UL	UL
37	DL	F	F	UL	UL	UL	UL	UL	UL	UL	UL	UL	UL	UL
38	DL	DL	F	F	UL	UL	UL	UL	UL	UL	UL	UL	UL	UL
39	DL	DL	DL	F	F	UL	UL	UL	UL	UL	UL	UL	UL	UL
40	DL	F	F	F	UL	UL	UL	UL	UL	UL	UL	UL	UL	UL
41	DL	DL	F	F	F	UL	UL	UL	UL	UL	UL	UL	UL	UL
42	DL	DL	DL	F	F	F	UL	UL	UL	UL	UL	UL	UL	UL

43	DL	DL	DL	DL	DL	DL	DL	DL	DL	F	F	F	F	UL
44	DL	DL	DL	DL	DL	DL	F	F	F	F	F	F	UL	UL
45	DL	DL	DL	DL	DL	DL	F	F	UL	UL	UL	UL	UL	UL
46	DL	DL	DL	DL	DL	F	UL	DL	DL	DL	DL	DL	F	UL
47	DL	DL	F	UL	UL	UL	UL	DL	DL	F	UL	UL	UL	UL
48	DL	F	UL	UL	UL	UL	UL	DL	F	UL	UL	UL	UL	UL
49	DL	DL	DL	DL	F	F	UL	DL	DL	DL	DL	F	F	UL
50	DL	DL	F	F	UL	UL	UL	DL	DL	F	F	UL	UL	UL
51	DL	F	F	UL	UL	UL	UL	DL	F	F	UL	UL	UL	UL
52	DL	F	F	F	F	F	UL	DL	F	F	F	F	F	UL
53	DL	DL	F	F	F	F	UL	DL	DL	F	F	F	F	UL
54	F	F	F	F	F	F	F	DL	DL	DL	DL	DL	DL	DL
55	DL	DL	F	F	F	UL	UL	UL	DL	DL	DL	DL	DL	DL
56-254	Reserved													
255	Slot configuration is provided to UE.													

Appendix 2 An example for SSB candidate locations with 15 kHz subcarrier spacing to get the maximum number of measurements. Number in coloured element refers the index of SSB.

Table 19. All possible candidate locations when $N_{\mathrm{SSB}}^{\mathrm{QCL}} = 1$ and UE can measure all eight cells and therefore eight beams. Colours shows measured locations.

Cell	Location	0	1	2	3	4	5	6	7	8	9
1		0	0	0	0	0	0	0	0	0	0
2		0	0	0	0	0	0	0	0	0	0
3		0	0	0	0	0	0	0	0	0	0
4		0	0	0	0	0	0	0	0	0	0
5		0	0	0	0	0	0	0	0	0	0
6		0	0	0	0	0	0	0	0	0	0
7		0	0	0	0	0	0	0	0	0	0
8		0	0	0	0	0	0	0	0	0	0

Table 20. An example of measured candidate locations when $N_{\mathrm{SSB}}^{\mathrm{QCL}} = 2$ and UE can measure 14 beams from seven cells. Colours shows measured locations.

Cell	Location	0	1	2	3	4	5	6	7	8	9
1		0	1	0	1	0	1	0	1	0	1
2		0	1	0	1	0	1	0	1	0	1
3		0	1	0	1	0	1	0	1	0	1
4		0	1	0	1	0	1	0	1	0	1
5		0	1	0	1	0	1	0	1	0	1
6		0	1	0	1	0	1	0	1	0	1
7		0	1	0	1	0	1	0	1	0	1
8											

Table 21. An example of measured candidate locations when $N_{\mathrm{SSB}}^{\mathrm{QCL}} = 4$ and UE can measure 14 beams from seven cells. Colours shows measured locations.

Cell	Location	0	1	2	3	4	5	6	7	8	9
1		0	1			0	1			0	1
2		0	1			0	1			0	1
3		0	1			0	1			0	1
4		0	1			0	1			0	1
5		0	1			0	1			0	1
6		0	1			0	1			0	1
7		0	1			0	1			0	1
8											

Table 22. An example of measured candidate locations when $N_{\mathrm{SSB}}^{\mathrm{QCL}} = 8$ and UE can measure 14 beams from seven cells. Colours shows measured locations.

Cell	Location	0	1	2	3	4	5	6	7	8	9
1		0	1							0	1
2		0	1							0	1
3		0	1							0	1
4		0	1							0	1
5		0	1							0	1
6		0	1							0	1
7		0	1							0	1
8											

Appendix 3 An example for SSB candidate locations with 30 kHz subcarrier spacing to get the maximum number of measurements. Number in coloured element refers the index of SSB.

Table 23. An example of measured candidate locations when $N_{\mathrm{SSB}}^{\mathrm{QCL}} = 1$ and UE can measure eight beams from eight cells. Colours shows measured locations.

Cell	Location	0	1	2	3	4	5	6	7	8	9	10	11	12	13	14	15	16	17	18	19
1		0	0	0	0	0	0	0	0	0	0	0	0	0	0	0	0	0	0	0	0
2		0	0	0	0	0	0	0	0	0	0	0	0	0	0	0	0	0	0	0	0
3		0	0	0	0	0	0	0	0	0	0	0	0	0	0	0	0	0	0	0	0
4		0	0	0	0	0	0	0	0	0	0	0	0	0	0	0	0	0	0	0	0
5		0	0	0	0	0	0	0	0	0	0	0	0	0	0	0	0	0	0	0	0
6		0	0	0	0	0	0	0	0	0	0	0	0	0	0	0	0	0	0	0	0
7		0	0	0	0	0	0	0	0	0	0	0	0	0	0	0	0	0	0	0	0
8		0	0	0	0	0	0	0	0	0	0	0	0	0	0	0	0	0	0	0	0

Table 24. An example of measured candidate locations when $N_{\mathrm{SSB}}^{\mathrm{QCL}} = 2$ and UE can measure 14 beams from seven cells. Colours shows measured locations.

Cell	Location	0	1	2	3	4	5	6	7	8	9	10	11	12	13	14	15	16	17	18	19
1		0	1	0	1	0	1	0	1	0	1	0	1	0	1	0	1	0	1	0	1
2		0	1	0	1	0	1	0	1	0	1	0	1	0	1	0	1	0	1	0	1
3		0	1	0	1	0	1	0	1	0	1	0	1	0	1	0	1	0	1	0	1
4		0	1	0	1	0	1	0	1	0	1	0	1	0	1	0	1	0	1	0	1
5		0	1	0	1	0	1	0	1	0	1	0	1	0	1	0	1	0	1	0	1
6		0	1	0	1	0	1	0	1	0	1	0	1	0	1	0	1	0	1	0	1
7		0	1	0	1	0	1	0	1	0	1	0	1	0	1	0	1	0	1	0	1
8																					

Table 25. An example of measured candidate locations when $N_{\mathrm{SSB}}^{\mathrm{QCL}} = 4$ and UE can measure 14 beams from four cells. Colours shows measured locations.

Cell	Location	0	1	2	3	4	5	6	7	8	9	10	11	12	13	14	15	16	17	18	19
1		0	1	2	3	0	1	2	3	0	1	2	3	0	1	2	3	0	1	2	3
2		0	1	2	3	0	1	2	3	0	1	2	3	0	1	2	3	0	1	2	3
3		0	1	2	3	0	1	2	3	0	1	2	3	0	1	2	3	0	1	2	3
4		0	1			0	1			0	1			0	1			0	1		
5																					
6																					
7																					
8																					

Table 26. An example of measured candidate locations when $N_{\mathrm{SSB}}^{\mathrm{QCL}} = 8$ and UE can measure 14 beams from four cells. Colours shows measured locations.

Cell \ Location	0	1	2	3	4	5	6	7	8	9	10	11	12	13	14	15	16	17	18	19
1	0	1	2	3					0	1	2	3					0	1	2	3
2	0	1	2	3					0	1	2	3					0	1	2	3
3	0	1	2	3					0	1	2	3					0	1	2	3
4	0	1							0	1							0	1		
5																				
6																				
7																				
8																				